

**Functional analysis of *Rim3* mutation that exhibits aberrant
epidermal morphogenesis**

By Shigekazu Tanaka

Doctor of Philosophy

Department of Genetics

School of Life Science

The Graduate University for Advanced Studies

2004

Contents

1. Abstracts

2. Introduction

3. Materials and methods

4. Results

4.1 Phenotype characterization of *GsdmA-3* mutant mice

4.1.1 *Rim3* mutant

4.1.1.1 *GsdmA-3* is expressed in supra basal cell layer of epidermis, and the expression starts at postnatal stage

4.1.1.2 Abnormal hair follicle development and disturbed hair cycle

4.1.1.3 Misdifferentiation of the epidermis and hair follicles

4.1.1.4 Hypertrophy of the upper hair follicular cells and the interfollicular epidermis

4.1.1.5 Atrophic sebaceous glands

4.1.1.6 Localization of the GsdmA proteins to plasma membrane

4.1.2 *M00745* mutant

4.1.2.1 *M00745* has a point mutation in *GsdmA-3*

4.1.2.2 Corneal opacity correlates to misdifferentiation of meibomian glands

4.2 Functional analysis of *GsdmA-3* using mice double heterozygous for *Rim3* and *Trp53* mutant alleles

4.2.1 Generation of double heterozygotes of *Rim3* and *Trp53* mutations

4.2.2 Incidence of spontaneous skin tumors in the double heterozygotes

4.2.3 Pathological analysis of the skin tumors developed in the double heterozygotes

4.2.4 Mouse GsdmA-1 and GsdmA-3, and human GSDMA proteins are downregulated in cutaneous tumors

5. Discussion

5.1 *GsdmA-3* controls proliferation and differentiation of bulge stem cells

5.2 The C-terminus domain is essential for the function of Gsdm/GSDM proteins

5.3 *GsdmA-3* regulates differentiation of sebaceous glands and meibomian glands

5.4 *GsdmA-3* is involved in suppression of skin tumors development

5.5 Molecular function of GsdmA-3 and other GsdmA/GSDMA proteins in regulation of proliferation and differentiation of epidermal cells

6. Acknowledgements

7. References

1. Abstracts

Two dominant mouse skin mutants, Recombinant-induced mutation 3 (*Rim3*) and Rex denuded (*Re^{den}*), arose spontaneously in different inbred strains, but exhibit very similar phenotype of hyperkeratosis and alopecia. Both mutants have a genetic alteration in GasderminA-3 (*GsdmA-3*), which is a member of novel gene family, *Gsdm*. The *Gsdm* family commonly share unique leucine-rich C-terminus domain, but the functions of *GsdmA-3* and *Gsdm* family are largely unknown.

In this study, to elucidate the function of *GsdmA-3* in the epidermal morphogenesis, I conducted analysis of spatiotemporal expression patterns of *GsdmA-3* and the related genes. In addition, I carried out in-depth characterization of the *Rim3* phenotype. The results indicated that *GsdmA-3* is specifically expressed in differentiated keratinocytes in epidermis after postnatal stage, but not in proliferating epidermal cells. Immunohistochemical analysis of BrdU-labeled epidermis revealed hyperproliferation and misdifferentiation of the upper follicular cells and the epidermis in the *Rim3* mutant. All the results suggested that *GsdmA-3* is involved in downregulation of cell-proliferation and differentiation of the epidermal stem cells.

As collaboration with a research group of National Cancer Institute, Tokyo, it was demonstrated that a human homologue *GSDMA* has a tumor suppressor activity. Mice heterozygous for *Trp53* knockout (*Trp53^{-/-}*) allele are known to frequently develop lymphomas, but never develop skin tumors. Although mice heterozygous for the *Rim3* mutation alone develop no skin tumors, I examined whether *GsdmA-3* is involved in tumor suppression in the *Trp53^{-/-}* genetic background. To do this, I generated mice

heterozygous for both of the *Rim3* and *Trp53* alleles. As a result, the double heterozygous mice (*GsdmA-3^{Rim3}/+*; *Trp53^{+/+}*) developed multiple metastatic squamous cell carcinomas (SCC) as early as 7 months of the age. In conjunction with the data that a human homologue *GSDMA* is a tumor suppressor for gastric cancer in human, this result suggested that *GsdmA-3* has a function to prevent tumor development in the mouse skin as well.

2. Introduction

Skin is the largest organ in the body. One of the key functions of skin is to serve a physical barrier, which protects internal organs from infections of many pathogens and from external environment. Skin, composed of epidermis and dermis, has appendages such as hair follicles, sebaceous and sweat glands. The barrier function is maintained by functions of these appendages, and its homeostasis is maintained by the balance between proliferation of stem cells and cell death following terminal differentiation.

The epidermal stem cells reside in both basal layer and bulge of hair follicles. While the stem cells in the basal layer differentiate into epidermal keratinocytes, those in the bulge give rise to not only hair follicles but also interfollicular epidermis and sebocytes in sebaceous glands (Cotsarelis *et al.*, 1990, 1999; Fuchs and Segre, 2000; Watt and Hogan, 2000; Lavker and Sun, 2000; Oshima *et al.*, 2001) (Figure 1A). Hair follicles undergo cycles of hair growth (anagen), regression (catagen) and quiescent (telogen) in adult stage (Hardy, 1992; Muller-Rover *et al.*, 2001) (Figure 1B). It is known that derangements of proliferation and differentiation of stem cells lead to cancer. It has been reported that β -catenin/Lef signaling controls differentiation of the bulge stem cells (Huelsenken *et al.*, 2001). It is, however, poorly understood what molecular mechanism regulates the proliferation and differentiation of the stem cells.

Mutant mice are powerful tools to study molecular mechanisms of development and morphogenesis at whole body level. To elucidate how proliferation and differentiation of epidermal stem cells are regulated, I analyzed several mouse mutants that show abnormal epidermal morphogenesis. Recombination-induced

mutation 3 (*Rim3*) spontaneously arose in National Institute of Genetics, and it exhibits dominant phenotype of hyperkeratosis and hair follicles degeneration. Another mutant Rex denuded (*Re^{den}*) shows phenotype very similar to *Rim3*. These two mutations were mapped to the same critical region in the mouse chromosome 11 (Sato *et al.*, 1998). It is already known that the two mutations have a genetic alteration in the C-terminus of the *GsdmA-3* gene. *Rim3* has a single base substitution, which leads to amino acid substitution, alanine to threonine. *Re^{den}* has 6 bases duplication, which leads to two amino acids apposition in the *GsdmA-3* protein (paper in preparation). Now, it is established that *GsdmA-3* is a member of the gene cluster referred to as *GsdmA*, which consists of direct tandem repeats of three homologous genes, *GsdmA-1*, *GsdmA-2* and *GsdmA-3* (paper in preparation). In the human syntenic region, there is only one homologous gene, *GSDMA*, and a structurally related *GSDMB* in the proximity of *GSDMA* (Figure 2A). Furthermore, *GsdmA* cluster is a member of novel gene family, *Gsdm/GSDM*. The *Gsdm* family is composed of *GsdmA/GSDMA*, *GSDMB*, *GsdmC/GSDMC* and *GsdmD/GSDMD* groups in mouse and human (Figure 2B, 2C) (paper in preparation). The *Gsdm/GSDM* family members commonly share unique leucine-rich C-terminus domain. The function of *Gsdm/GSDM* family as well as the novel leucine-rich motif is largely unknown.

In this study, to elucidate the function of *GsdmA-3* in the epidermal morphogenesis, I conducted expression analysis of *GsdmA-3* and in-depth characterization of the *Rim3* phenotype. The results indicated that *GsdmA-3* is expressed only in skin, and that *Rim3* mice showed hyperproliferation and misdifferentiation of

epidermal stem cells. Furthermore, I carried out genetical analysis of another mouse mutant, *M00745*, which was generated by the RIKEN ENU-mutagenesis project and exhibits phenotype resembling the *Rim3* and *Re^{den}* mutants. As a result, it appeared that *M00745* has a nonsense mutation that causes truncation of the very end of the conserved C-terminus of the GsdmA-3 protein. All the result suggested that *GsdmA-3* is involved in a genetic pathway that regulates proliferation and differentiation of mouse epidermal cells.

GSDMA, a human homologue of *GsdmA* cluster, is located at the human chromosome 17q12 region. That region is frequently amplified in human gastric cancer and breast cancer (Bieche *et al.*, 1996; Kokkola *et al.*, 1997), and is called 17q12 amplicon. Amplification of *ERBB2* in the amplicon was observed in different kinds of cancers (Stein *et al.*, 1994), and thought to be a cause of tumor development (Xie *et al.*, 1999; Kiguchi *et al.*, 2000). In contrast, it is known that tumor suppressor genes are frequently deleted or silenced by methylation of the promoter in many cancers (Merajver *et al.*, 1995; Li *et al.*, 2002). As collaboration with Dr. H. Sasaki of National Cancer Institute, Tokyo, it was demonstrated that the human homologue *GSDMA* was silenced by DNA methylation in gastric cancers (paper submitted). Furthermore, it appeared that over-expression of the *GSDMA* leads growth inhibition and apoptosis of cancer cells, indicating that *GSDMA* is a tumor suppressor (paper submitted).

There are several lines of evidence that model mice harboring oncogenic transgenes commonly developed tumors in non-hairy skin. For example, transgenic mice with over expression of the *Gli2* gene in skin, which encodes a key transcription

factor in the Shh signaling, spontaneously develop basal cell carcinoma in non-hairy skins such as ear, tail and dorsal paws (Grachtchouk *et al.*, 2000). Likewise, transgenic mice with constitutive expression of the stabilized β -catenin develop trichofolliculomas and pilomatricomas in non-hairy skins (Gat *et al.*, 1998). Since mutations of *GsdmA-3* cause hyperproliferation of epidermis and the expression of *GsdmA-3* is restricted to hairy skin, we hypothesized that the function of the wild-type *GsdmA-3* gene is involved in tumor suppression *in vivo*. Tumorigenesis is multistep process with accumulating genetic alterations (Wu and Pandolfi, 2001). It is known that mutations of *Trp53* are an early event of skin tumors, and *Trp53* mutated cells are precancerous (Jonason, et al., 1996; Delfino, et al., 2002). Therefore, I generated mice heterozygotes for both *Rim3* and *Trp53* alleles. As a result, the double heterozygous mice (*GsdmA-3*^{*Rim3*}/+; *Trp53*^{+/+}) showed significantly high incidence of metastatic squamous cell carcinomas (SCC). I also found that the expression of *GsdmA-3* is diminished or lost in the skin tumors. These results suggested that *GsdmA-3* is involved in a pathway that downregulates proliferation of epidermal stem cells and regulates tumor suppression in the mouse skin.

3. Materials and methods

Mice

Recombination-induced mutation 3 (*Rim3*) arose spontaneously in C57BL/10J strain harboring a recombinant MHC. The mutant strain, C57BL/10J-*Rim3*, has been maintained in Mammalian Genetics Laboratory of National Institute of Genetics (NIG, Mishima, Japan), and maintained in NIG by repeating backcrosses to C57BL/10J strain that was originally purchased from the Jackson Laboratory (Bar Harbor, Maine, USA). *M00745* mutant was generated in C57BL/6J by N-ethyl-N-nitrosourea (ENU) mutagenesis in RIKEN Genomic Sciences Center (RIKEN GSC) (Yokohama, Japan). *Trp53* knockout mouse was originally produced by Dr. Aizawa of RIKEN Life Science Center (Tsukuba, Japan) (Tsukada, *et al.*, 1993), and was obtained through Dr. Kyoji Hioki of Central Institute for Experimental Animals (Kawasaki, Japan). The mice were maintained by repeating backcrosses to C57BL/6J strain in NIG. Japanese Fancy mouse-1 (JF1) strain was established and maintained in NIG.

RT-PCR

Samples from various organs were homogenized in Isogen (Nippon gene, Tokyo, Japan), and total RNA was extracted following the manufacturer's recommendations. cDNAs were synthesized from the total RNA according to the manufacturer's manual (GIBCO-BRL, Superscript kit). The cDNAs of *GsdmA-1*, *GsdmA-3* and glyceraldehyde-3-phosphate dehydrogenase (*Gapdh*) were amplified by the polymerase chain reaction (PCR) with following primer pairs, *GsdmA-1* (forward, 5'-

CACCCTTCCCTGAGACAATG-3'; Reverse, 5'-CACACCATAACCACCACCAT-3'),
GsdmA-3 (forward, 5'-CCAAACACCTGCTGCTGAACA-3'; reverse, 5'-
ACTTTTACTCCCTGCCATTAG-3') and GAPDH (forward, 5'-
TGAAAGGTGAGTGGGAGGAAT-3'; reverse, 5'-
GATGTAGGCCATGAGGTCCACCAC-3'). These primers were purchased from
RIKAKEN Co. Ltd. (Nagoya, Japan).

Sample preparation for histological analysis

Samples for histological analysis were prepared essentially following the method of Paus *et al.* (1999). Back skin was isolated from wild-type and *Rim3*^{+/+} litter mates, and fixed in 4% paraformaldehyde (PFA) in phosphate buffered saline (PBS) at 4°C for over night. The skin was minced into rectangle pieces (5 × 10 mm), replaced in either 70% ethanol for paraffin section or 30% sucrose in RNase-free distilled water (DW) for cryosection. In paraffin sections, samples were embedded in paraffin by FTP-150C (Sakura Finetechnical Co. Ltd., Tokyo, Japan), and sectioned at 5 μm using rotary microtome 2065 Supercut (Leica microsystems Co. Ltd., Tokyo, Japan). For cryosections, samples were embedded in Optimal Cutting Temperature (O.C.T) compound, (Sakura Finetechnical Co. Ltd., Tokyo, Japan), frozen in liquid nitrogen and sectioned at 25 μm by CM1510 (Leica microsystems Co. Ltd., Tokyo, Japan). Cryosections were preserved at -20°C.

***In situ* hybridization**

To detect the expression of *GsdmA-1* and *GsdmA-3*, *in situ* hybridization was performed on skin cryosections. Sampling procedure was as described above. Cryosections were hybridized with digoxigenin-labeled riboprobes transcribed *in vitro* according to the manufacturer's manual (Roche, Tokyo, Japan). *GsdmA-1* cRNA probe that has high homology to *GsdmA-3* was used in hybridization.

Antibody

Following primary antibodies, Anti-Keratin 6 (K6) (1:50, BAbCO), anti-Keratin 10 (K10) (1:50, BAbCO), and anti-Keratin 14 (K14) (1:50, BAbCO) were purchased from Covance Research Products Inc. (Denver, U. S. A). Chicken polyclonal anti-GsdmA antibodies were produced for following two peptides. Anti-GsdmA-1 (37) was raised for a peptide CLVLRKRKSTLF of GsdmA-1, and Anti-GsdmA-3 (246) was raised for a peptide QMISEEPREEKLG of GsdmA-3 (Figure 2C, Magenta boxes). These antibodies were made by Asahi Technoglass Co. Ltd. (Funabashi, Japan). As the secondary antibodies, Alexa Fluor 488-conjugated anti-mouse IgG (1:500) (Molecular Probes), fluorescein isothiocyanate (FITC)-conjugated donkey anti-chicken IgY (1:500) (Jackson ImmunoResearch), peroxidase-conjugated donkey anti-chicken IgY (1:500) (Jackson ImmunoResearch), were purchased and used in this study.

Histological analysis and immunohistochemistry

Hematoxylin and Eosin (HE) staining: Back skin of wild-type, *Rim3/+* and *M00745/+* mice of the same litter mates were prepared as described above. Paraffin was removed from the sections by rinse in 100% xylene for 5 minutes at three times, and the sections were hydrated progressively in 100%, 90%, 80%, 70% ethanol series for 5 minutes at each step. The sections were stained with hematoxylin (Wako, Japan) for 5 minutes. After washing with running water for more than 30 minutes, stained with eosin (Muto Pure Chemicals Co. Ltd, Japan) for 1 minute. Then the sections were dehydrated progressively in 70%, 80%, 90%, 100% ethanol series for 5 minutes at each steps, and dehydrated in 100% xylene for 5 minutes at three times. These procedures were done at room temperature.

Immunofluorescence: Skin samples were fixed with 4% PFA and embedded in paraffin. Paraffin was removed from section, and the sections were hydrated with same conditions as described above. Paraffin sections were microwaved in 10 mM sodium citrate buffer (pH 6) for 5 minutes to unmask the antigen. After washing in water, the sections were blocked in 5% bovine serum albumin (BSA) in PBS for 1 hour at 4°C, and were washed in PBS for 5 min at three times. Then the sections were hybridized with the primary antibodies at 4°C for over night. After washing in PBS, the sections were hybridized with secondary antibodies for 1 hour at room temperature and counterstained with 4,6-diamino 2-phenylindole (DAPI). These sections were analyzed and photographed using fluorescence microscope BX51 (OLYMPUS, Tokyo, Japan), or

a confocal fluorescence microscope FV500 (OLYMPUS, Tokyo, Japan) or a LSM510 (Carl Zeiss, Germany).

DAB staining: Paraffin was removed from sections, and the sections were hydrated with same conditions as described above. The paraffin sections were treated with trypsin (1 mg/ml) for 5 minutes at 37°C to unmask the antigen. After washing in water, endogenous peroxidase activity was quenched with 0.3% hydrogen peroxide in methanol for 30 minutes. After washing in PBS, the sections were blocked in 5% BSA in PBS for 1 hour at 4°C, and were incubated with the primary antibodies at 4°C over night. After washing in PBS, the sections were incubated with primary antibodies at 4°C over night. After washing in PBS, the sections were incubated with the secondary antibodies at room temperature for 1 hour. The antibody-antigen reaction was visualized by DAB staining. Following solution was used in DAB staining: 1 mg/ml 3,3'-diaminobenzidine-4HCl (DAB) (Wako, Japan) in 0.02% hydrogen peroxide and 0.1 M Tris-HCl (pH 7.2).

BrdU labeling

For proliferation assay, wild-type and *Rim3*^{+/+} mice of the same litter mates were injected with 50 mg/g body weight 5-Bromodeoxyuridine (BrdU) (Sigma, Japan), and the skin samples were recovered 2 hours after injection, and processed as described above. Paraffin sections were incubated with mouse monoclonal anti-BrdU antibody (1:500) (Sigma, Japan). Signals of anti-BrdU antibodies were detected by ABC method using Mouse IgG VECTASTAIN ABC kit (Vector Laboratories, U. S. A), following the

manufacturer's recommendations and by DAB staining as described above. I made following modification. Before trypsin treatment, sections were washed in 2N HCl in PBS at 37°C for 20 minutes to denature DNA, and rinsed in 0.1 M Tris-HCl (pH7.5) for 5 minutes at two times.

Oil Red O staining

Frozen sections were prepared as described above. They were washed in distilled water and stained by Oil Red O staining solution (300 mg Oil Red O, SIGMA O-0625, in 100 ml isopropanol) for 15 minutes at room temperature. The sections were then washed in 60% isopropanol in distilled water and in PBS, and counter-stained with hematoxylin.

Immunoelectron microscopy

Back skins from 12 days-old wild-type and *Rim3*^{+/+} mice were minced into 2 mm square pieces. These samples were left in the fixative solution (4% paraformaldehyde, 0.1% glutaraldehyde, 0.1 M cacodylic acid) at 4°C for 2 hours. The samples were dehydrated progressively in 50–100% ethanol for 30 minutes at –20°C at each step. Then samples were embedded in Lowicryl K4M, and dissected by ultramicrotome. The thin sections were blocked with 1% BSA in PBS, and 1.5% goat serum at room temperature for 15 minutes, and then incubated with the primary antibody (chicken polyclonal anti-GsdmA) at 4°C for overnight. The sections were then stained with the secondary antibodies, gold particle (10 nm) conjugated anti-chicken IgG (1/20, 1%BSA-PBS), at 4°C overnight. Ultra-thin sections were contrasted with uranyl acetate and lead citrate,

and analyzed and photographed by a JEOL JEM2000EX at 120kV (J. E. O. L., Tokyo, Japan). Observation by immunoelectron microscopy was done by Hanaichi UltraStructure Research Institute (HUSRI, Okazaki, Japan).

Linkage analysis of the *M00745* mutation

Heterozygotes of *M00745* were mated with JF1 mice, and the F₁ progeny with the phenotype were backcrossed to JF1 mice. For mapping of the phenotype, the backcross progeny were phenotyped, and genomic DNA was prepared from their tails. *GsdmA* linked four microsatellite markers, *D11MIT236*, *D11MIT70*, *D11MIT124*, *D11MIT132*, and *GsdmC* and *GsdmD*-linked two markers, *D15MIT11*, *D15MIT73*, were used for genotyping for the DNAs of the backcross progeny.

Sequencing of coding regions of the *GsdmA-1* and *GsdmA-3* genes of *M00745* mutant

To analyze sequence of *GsdmA-1* and *GsdmA-3* in the *M00745* mutant, full length cDNA of *GsdmA-1* and *GsdmA-3* were cloned into pGEM-Teasy Vector (Promega, Tokyo, Japan). Following primers were used for sequencing:

T7: (5'-GTAATACGACTCACTATAGGGCGA-3');

Sp6: (5'-TATTTAGGTGACACTATAG-3');

GDA1Seq341F: (5'-GCTCGAGTAGAGGGAGATGT-3');

GDA1Seq731F: (5'-GATGAGTGGGGCATTCCACA-3');

GDA1Seq1310R: (5'-GGCCGCTTAGTCCCACCAGT-3');

GDA1Seq1610R: (5'-TTAGTGGGTGCTGAGCTGGA-3');

GDA3Seq301F: (5'-GACAGACAGTGGCAACTTTA-3');

GDA3Seq701F: (5'-CGAGTGAGACTACTGAGAGT-3');

GDA3Seq1440R: (5'-CTGCTTAGCAGGTGAAGGAG-3').

These primers were purchased from RIKAKEN Co. Ltd. (Nagoya, Japan) and Invitrogen (Tokyo, Japan).

Generation of mice heterozygous both for *Rim3* and *Trp53* KO (*p53*⁻) alleles

To generate mice double heterozygous for *Rim3* and *Trp53*⁻ alleles, I crossed *Rim3* heterozygotes (*GsdmA-3^{Rim3}/+*) to *Trp53*⁻ heterozygotes (*Trp53*⁻/+).

Genotyping of *Trp53* knockout (*Trp53*⁻) allele

To genotype *Trp53* alleles, I used following primer pairs, *neo* (forward, 5'-CTTGGGTGGAGAGGCTATTC-3'; reverse, 5'-AGGTGAGATGACAGGAGATC-3') and *Trp53* (forward, 5'-ATAGGTCGGCGGTTCAT-3'; reverse, 5'-CCCGAGTATCTGGAAGACAG-3'). The information of the primer sequences and the PCR condition were obtained from the database of Jackson Laboratory (<http://www.jax.org/>). These primers were purchased from Invitrogen (Tokyo, Japan).

Localization of GSDMA protein in human samples

Human normal skin sections and human SCC skin sections were purchased from BioChain Institute Inc. (Hayward, U. S. A.). These sections were stained with anti-

GsdmA as described above.

4. Results

4.1 Phenotype characterization of *GsdmA-3* mutant mice

4.1.1 *Rim3* mutant

4.1.1.1 *GsdmA-3* is expressed in supra basal cell layer of epidermis, and the expression starts at postnatal stage

It was reported that *GsdmA-1* is expressed in skin and stomach (Saeki *et. al.*, 2000). Expression pattern of *GsdmA-3* had been, however, unknown until this study. Therefore, I first examined spatiotemporal expression patterns of *GsdmA-3* in wild-type mice by reverse transcription-PCR (RT-PCR). The result clearly showed that *GsdmA-3* is only expressed in skin, but not other organs (Figure 3A). The expression of *GsdmA-1* starts from E15.5, whereas the expression of *GsdmA-3* starts from postnatal stage, and its expression level gradually increased thereafter (Figure 3B).

I also carried out *in situ* hybridization with the probe that detects both *GsdmA-1* and *GsdmA-3* mRNA. In wild-type mice, *GsdmA-1* and/or *GsdmA-3* are expressed in supra basal cell layer of epidermis (black arrows, Figure 4A and 4C), sebocytes in sebaceous glands (white arrows, Figure 4A and 4E) and inner root sheath (IRS) of hair follicles (arrowheads, Figure 4A and 4G). In *Rim3*^{+/+} mouse, *GsdmA-1* and/or *GsdmA-3* are similarly expressed in the supra basal cell layer of epidermis (black arrows, Figure 4B and 4D), and inner root sheath (IRS) of hair follicles (arrowheads, Figure 4B and 4H). Because the sebaceous glands were degenerated (Figure 4F), I could not observe the expression of *GsdmA-1* and/or *GsdmA-3* in the sebocytes in *Rim3*^{+/+} mouse.

4.1.1.2 Abnormal hair follicle development and disturbed hair cycle

I examined whether degeneration of the hair follicles in *Rim3* depends on the hair cycle. Sagittal sections of the dorsal skin of wild-type and the *Rim3*^{+/+} mice at 1 month, 3 months and 10 months of age were stained with hematoxylin and eosin. The result showed that developmental stage of the hair follicle is synchronized in the wild-type mouse through all the ages (arrowheads in Figure 5A, 5D and 5G). The gross phenotype of the *Rim3*^{+/+} mouse at different age is shown in the right side in Figure 5. In the *Rim3*^{+/+} mouse at 1 month of age, the dermal papillas were formed in different directions (arrowheads in Figure 5B), and keratins were accumulated in the upper hair follicles (arrows in Figure 5B). Anagen phase and abnormal catagen phase coexisted in the *Rim3*^{+/+} mouse at 3 months of age (arrowhead and asterisk in Figure 5E, respectively). Finally, all hair follicles were completely lost in the *Rim3*^{+/+} mouse at 10 months of age (Figure 5H). These results suggest that the hair cycle is disturbed in the *Rim3*^{+/+} mice.

4.1.1.3 Misdifferentiation of the epidermis and the hair follicles

To analyze how the epidermal cells in *Rim3*^{+/+} mice differentiate, I carried out immunohistochemical analysis using the epidermal layer-specific antibodies. Sagittal paraffin sections of the dorsal skin of wild-type and the *Rim3*^{+/+} mice at 3 months of age were stained with anti-keratin antibodies. Staining with anti-K14 antibody detected basal cell layer and outer root sheath (ORS) in the wild-type skins (arrows in Figure 6A). In *Rim3*^{+/+}, I observed hyperplasia of epidermal and follicular cells (arrows in Figure

6B). Keratin 10 (K10) is an epidermal marker of terminal differentiation. Staining with anti-K10 antibody detected only granular layer in the wild-type mouse, but ectopic expression of K10 was observed in the upper hair follicles in the *Rim3/+* mouse (arrow in Figure 6D). Keratin 6 (K6) is a marker of ORS and wounding epidermis (Mansbridge and Knapp, 1987). In the *Rim3/+* mouse, K6 expression was observed in hair follicles and epidermis (arrows in Figure 6F). Thus, it appeared that *Rim3/+* mice showed hyperproliferation and misdifferentiation of epidermis and hair follicular cells.

4.1.1.4 Hyperproliferation of the upper hair follicular cells and interfollicular epidermis

To characterize the proliferation of epidermal cells, the proliferating cells in the basal layer and the hair follicles were labeled by BrdU labeling (arrows in Figure 7A and 7B). In the *Rim3/+* mouse at 3 months of age, an increased number of the BrdU-positive cells was observed in the upper hair follicles and the interfollicular epidermis near the hair follicles, as compared with those of the wild-type mouse (arrows in Figure 7A and 7B). The result showed hyperproliferative nature of the upper hair follicular cells and the interfollicular epidermis in *Rim3/+* mice.

4.1.1.5 Atrophic Sebaceous glands

Expression of *GsdmA-1* and/or *GsdmA-3* was observed in sebaceous glands. Therefore, to analyze whether sebaceous glands are affected in *Rim3/+* mice, I examined sebaceous glands by Oil Red O staining. I found that there were almost no sebocytes in

the *Rim3/+* mouse at 3 months of age (Figure 8B). This suggested that the progeny cells do not differentiate into sebocytes in *Rim3/+* mice, after moving out of the bulge.

4.1.1.6 Localization of the GsdmA proteins to plasma membrane

To analyze localization of GsdmA proteins, I generated polyclonal antibodies against to GsdmA-1 and GsdmA-3 by immunizing chicks with synthesized peptides of each protein. The produced polyclonal antibodies, however, cross hybridize with each other, and I couldn't distinguish the GsdmA-3 from the GsdmA-1 by the antibodies. The result of hybridization with the antibodies indicated that GsdmA-1 and/or GsdmA-3 are expressed in epidermis, sebaceous glands and hair follicles of wild-type and *Rim3/+* mouse (Figure 9A and 9B). In the epidermis of the wild-type and *Rim3/+* mice, dotted signals of GsdmA proteins are localized to cytoplasm and plasma membrane of supra basal layers (arrow, Figure 9C and 9D). GsdmA proteins are not localized to cell membrane that contacted with basal cells (Figure 9C and 9D). In the *Rim3/+* mouse, dotted signals of GsdmA proteins tends to be localized to cytoplasm (Figure 9F), whereas in the wild-type mouse, the signals are mostly localized to cell membrane (Figure 9E). In sebocytes of the wild-type mouse, the GsdmA proteins were rather uniformly scattered in cytoplasm (Figure 9G).

To examine relationship between the localization of GsdmA proteins and proliferation activity of cells, I carried out double staining of the BrdU-labeled wild-type and *Rim3/+* skin with anti-GsdmA and anti-BrdU antibodies. The result clearly showed that GsdmA-positive cells do not overlap BrdU-positive proliferating cells,

indicating that proliferative cells don't possess GsdmA proteins (Figure 10A and 10B).

In electron microscopic observation, the plasma membrane of all layers in the inner root sheath (IRS), especially in Henle's (He) layer, was labeled with gold particles in the wild-type mouse (arrows in Figure 11B). In the high magnification, the particles were observed in the vesicles (arrowheads in Figure 11B) and organelles (arrows, Figure 11C). In sebocytes, the particles were specifically detected in unknown high-density granules (arrow in Figure 11D and 11E).

4.1.2 *M00745* mutant

4.1.2.1 *M00745* has a point mutation in *GsdmA-3*

A dominant skin mutant *M00745* was generated by the ENU-mutagenesis project of RIKEN Genomic Sciences Center, and it exhibits scarring alopecia resembling the phenotype of *Rim3* and *Re^{den}*. First, I carried out linkage analysis based on totally 70 backcross progeny generated from a backcross of (*M00745/+* X JF1) F₁ to JF1. This inter-subspecific backcross revealed tight linkage of the *M00745* mutant gene to a marker *D11Mit124* and the *GsdmA* cluster (Figure 12A). Sequencing of the *M00745* mutant revealed a point mutation in *GsdmA-3*, but not in *GsdmA-1*. This single base-substitution T1408A in exon 11 of *GsdmA-3* changes the codon442 for Tyrosine to the Stop codon (Figure 12B). The amino acid sequence A-L-Y including the Tyrosine442 is conserved among all members of the Gsdm family (Figure 2C). The *M00745* mutation gives rise to truncated GsdmA-3 protein that lacks 22 amino acids of the very end of the C-terminus.

4.1.2.2 Corneal opacity correlates to misdifferentiation of meibomian glands

To elucidate phenotypic difference of two mutations, *Rim3* and *M00745*, I employed histological analysis of the two mutant mice. Degenerated hair follicles, atrophy of sebaceous glands, hyperproliferation of epidermis and hair follicles were observed in the both mutants, but epidermis of *M00745/+* mice was much thicker than that of the *Rim3/+* mouse (Figure 13). Another difference observed between *Rim3/+* and *M00745/+* mice was late-onset corneal opacity. *Rim3/+* mice exhibited corneal opacity after 3 months of age (Sato, *et al.*, 1998) (Figure 14D and 14F), whereas *M00745/+* mice did not even after 10 months of age (Figure 14G). Eyelids have modified sebaceous glands, referred to as meibomian glands, which secrete meibum, the oily material, which prevents corneal surface of eyes from drying out (Tiffany, 1985). I found that meibomian glands of the *Rim3/+* mouse were cystic and seemed to be dysfunctional, but *M00745/+* mouse has cells containing meibum (Figure 15E, 15F and 15G). It suggested that meibum lipid is depleted in *Rim3/+*, but not in *M00745/+*. The affected structure of the meibomian glands may explain the late-onset corneal opacity specifically observed in *Rim3/+* mice (Figure 14 and 15).

A higher magnification of the meibomian glands of the *M00745/+* mouse at 10 months of age showed an ectopic hair-like structure in the meibomian glands (white arrowheads in Figure 15H), suggesting abnormal differentiation of the stem cells in the meibomian glands in *M00745* mutant mouse. Difference of the phenotypes between *Rim3/+* and *M00745/+* mice may be attributable to difference of the mutation type in

GsdmA-3. It is also possible that different genetic background of the *Rim3*^{+/+} and *M00745*^{+/+} is responsible for the difference.

4.2 Functional analysis of *GsdmA-3* using mice double heterozygous for *Rim3* and *Trp53*⁻ mutant alleles

4.2.1 Generation of double heterozygotes of *Rim3* and *Trp53* mutations

As collaboration with Dr. H. Sasaki of National Cancer Institute, Tokyo, it was demonstrated that a human homologue of *GsdmA* cluster genes, *GSDMA*, has a tumor suppressor activity (paper submitted). Furthermore, this study indicated that mutations of *GsdmA-3* results in hyperproliferation of epidermal cells. Therefore, I intended to test whether *GsdmA-3* has tumor suppressor activity or whether it is involved in a pathway of tumor suppression. In human, several skin tumors frequently have mutations in Transformation related protein 53 (*Trp53*) gene (Giglia-Mari and Sarasin, 2003). Mice heterozygous for *Trp53* knockout allele (*Trp53*⁻) are known to predominantly develop lymphomas, but never develop skin tumors without chemical or physicochemical induction (Donehower, *et al.*, 1992). *Rim3*^{+/+} mice scarcely develop skin tumors except that they are over 20 months of age (data not shown). To examine whether *GsdmA-3* deficient mice are susceptible to skin tumor induction, I generated mice heterozygous both for *Rim3* and *Trp53*⁻ alleles. As *GsdmA-3* and *Trp53* are linked on the mouse chromosome 11, the *Rim3*^{+/+} mice were crossed to *Trp53*⁻ heterozygotes, and the progeny mice that harbored both mutant alleles were used in the later experiment.

4.2.2 Incidence of spontaneous skin tumors in the double heterozygotes

The tumor incidence was assessed by monitoring spontaneous skin tumor development in mice generated from the cross of *Rim3*^{+/+} and *Trp53*^{+/+} mice. Cumulated incidence of skin tumors in the mice with each of the four different genotypes was obtained by observation for 12 months of time course after birth (Figure 16). The double heterozygous mice (*GsdmA-3*^{*Rim3*}^{+/+}; *Trp53*^{+/+}) began to develop grossly visible skin tumors around 7 months of age. The tumors were multiple and predominantly observed in the head and neck, but merely observed in the trunk and buttock (Table 1, Figure 17C and 17D). By 12 months, 80 % (17 of 21) of the double heterozygous mice developed tumors. In contrast, mice heterozygous for single *Trp53* mutation never develop skin tumors (0 of 20), although they developed a few non-skin tumors. The frequency of the visible skin tumors developed in the double heterozygous mice was remarkably higher than those in the two other single heterozygous mice, *Rim3*^{+/+} and *Trp53*^{-/-}. This result suggested that function of *GsdmA-3* is involved in tumor suppression in mouse skin.

4.2.3 Pathological analysis of the skin tumors developed in the double heterozygotes

Pathological analysis was carried out for the skin tumors developed in the double heterozygotes of *Rim3* and *Trp53* mutations. Macroscopic observation indicated that some tumors were grossly similar to human keratoacanthoma (KA) with characteristics of hemispheric and smooth tumor and a horny plug in the center (Figure 17A and 17B). The KA-like mouse tumors included keratinized cells surrounded by low atypical

squamous cells. Invasion of tumor cells into dermis was not seen in these KA-like tumors. The double heterozygotes also develop multiple tumors, histology of which was very similar to human squamous cell carcinoma (SCC). These SCC-like tumors were developed in the head and neck (Figure 17C, 17D and 17E). They exhibited dyskeratosis and proliferation of squamous cells with various size of nuclear and formed many horn pearls (arrows in Figure 17I). I observed invasion of the tumor cells into deeper structures. Furthermore, lymph nodes at the periphery of the SCC-like tumors included well-differentiated metastatic squamous cell carcinoma (Figure 17J).

4.2.4 Mouse GsdmA-1 and GsdmA-3 and human GSDMA proteins are downregulated in skin tumors

To elucidate relationship between the expression of GsdmA-3 and tumor development, I examined localization of GsdmA-3/GSDMA proteins in the skin tumors. Skin tumors developed in the double heterozygous mice and sections of human SCC were stained with anti-GsdmA antibody. At the same time, I examined the expression pattern of the GsdmA-3/GSDM proteins in normal skins of mouse and human as control experiment. The localization of the GsdmA-3 proteins in normal mouse skin was already described in this thesis (see section 4.1.1.5). In human normal skin, GSDMA protein is intensely localized in granular layer, and weakly detected in plasma membrane of spinous layers (black arrows in Figure 18B). The GsdmA-1 and/or GsdmA-3 proteins were localized in sebaceous glands in mouse skin, but human GSDMA was not detected in sebaceous glands (white arrows in Figure 18C). It may indicated that GsdmA-3, but not GsdmA-1,

is expressed in mouse sebaceous glands, because the amino acid sequence of human GSDMA is much more similar to the mouse GsdmA-1 than to GsdmA-3.

In human, ductal epithelium (arrows in Figure 18D and 18E) and intra-ductal component of sweat glands (white arrows in Figure 18E) were also densely stained by anti-GsdmA antibody. In mouse, sweat glands only exist in foot pads. The expression of GsdmA-1 and/or GsdmA-3 in mouse sweat glands is not examined in this study.

In the double heterozygous mouse that developed SCC, the supra basal layers in the hyperplastic epidermis adjacent to the SCC were stained with anti-GsdmA antibody (Figure 19A). Neoplastic cells in the SCC are not stained (Figure 19B), but keratinized cells (arrowheads in Figure 19B) are weakly stained. Likewise, in human SCC, supra basal layers in the hyperplastic epidermis adjacent to the SCC were stained with the same antibody (Figure 19C). Localization of GSDMA shows polarity; the signals of the antibodies become stronger toward the superficial layer (arrowheads in Figure 19C). In human SCC that is invading dermis, neoplastic cells are not stained with the anti-GsdmA antibody (Figure 19D).

Serial sections of the hyperplastic epidermis in the double heterozygous mouse with SCC were stained with HE or the anti-GsdmA antibody. Notably, localization of GsdmA proteins was changed depending on stages of epidermis differentiation, which can be monitored by the nuclear staining with HE. The GsdmA protein(s) was absent in the basal layer (white arrowheads in Figure 20A and 20B). The proteins appeared in the membrane of cells during differentiation stage (asterisk in Figure 20A and 20B), and in the cytoplasm of the terminal differentiated cells (arrowheads in Figure 20A and 20B).

5. Discussion

5.1 *GsdmA-3* controls proliferation and differentiation of bulge stem cells

Previous study of our group had shown that the two mouse mutations, *Rim3* and *Re^{den}*, are mapped to the same region in chromosome 11, and that they exhibit similar phenotype such as hyperkeratosis and corneal opacity (Sato *et al.*, 1998). Before I started this study, it was revealed that *Rim3* and *Re^{den}* have a missense mutation and an apposition of two amino acids in the *GsdmA-3* gene, respectively. However, the function of *GsdmA-3* had been largely unknown, because in-depth characterization of the phenotype of the two mutants had not been done until this study. In a separate study of our group, it was also established that *GsdmA-3* is a member of novel gene family, *Gsdm* (Tamura *et al.*, paper in preparation). The *Gsdm* family commonly share unique leucine-rich C-terminus domain. Again, the function of the motif and the function of the member of the *Gsdm* family were unknown.

I have extended the previous studies of our group in order to elucidate the biological function of the *GsdmA-3* gene. I took two approaches to reveal the function of *GsdmA-3*. First, I carried out thorough characterization of the phenotype of the *GsdmA-3* mutants. Second, I analyzed detailed expression pattern of the mouse *GsdmA-3* and the human homologue *GSDMA* both in normal skins and skin tumors. The present studies showed that mouse *GsdmA-3* and human homologue *GSDMA* are expressed in differentiated keratinocytes in supra basal cell layer of epidermis and in hair follicles, but not in proliferating cells in basal cell layer, as well as neoplastic cells. The expression of *GsdmA-3* starts at postnatal stage, and thereafter increased gradually.

Since the three mouse mutants of *GsdmA-3* similarly exhibit hyperplastic epidermis and misdifferentiation of the epidermal cells, *GsdmA-3* likely functions to downregulate proliferation of epidermal stem cells, and to regulate differentiation of epidermal cells.

I found that BrdU positive cells reside in the basal layer from the upper follicular to interfollicular epidermis in *Rim3/+* mice at 3 months of age. (Figure 6H). It is known that bulge stem cells migrate bi-directionally; upward to epidermis and downward to lower follicular epidermis. Therefore, the *Rim3* phenotype was likely caused by unidirectional upward migration of proliferating cells from the bulge to the epidermis (Figure 21). Since in *Rim3/+* mice BrdU positive cells are less frequently observed in the center of the interfollicular epidermis, but more frequently in the epidermis closer to the follicles, it is conceivable that the *Rim3* mutation affects property of the bulge stem cells in hair follicles, but not property of the stem cells in basal layer of epidermis. I observed ectopic expression of K10, which is an interfollicular epidermal marker, in the follicular epidermis of *Rim3/+*. The hair follicles no longer maintain the tubular structure by switching of morphogenetic program from follicular epidermis to interfollicular epidermis. Finally, the hair follicles are degenerated in *Rim3/+* mice. All the results in this study, thus, suggested that *GsdmA-3* regulates cell lineage from bulge stem cells.

It was reported that Wnt signaling regulates cell lineage of bulge stem cells (Merrill, *et al.*, 2001; Huelsken, *et al.*, 2001; DasGupta, *et al.*, 2002; Niemann, *et al.*, 2002). When function of β -catenin is conditionally knockout in mouse epidermis from postnatal stage, the bulge stem cells can only differentiate into the epidermal lineage

(Huelsenken, *et al.*, 2001). It was reported that over-expression of delta-N Lef1 that lacks β -catenin binding sites in the epidermis leads to hair loss from 6 weeks of age and developed spontaneous tumors (Niemann, *et al.*, 2002). That report indicated that hair follicular keratinocytes undergo differentiation into interfollicular epidermis. The phenotype of the above knockout mutant mice closely resembles that of *Rim3* in that differentiation of the bulge stem cells into the epidermis is affected. Therefore, it is possible that *GsdmA-3* is involved in inhibition of β -catenin signaling via Lef1 in epidermis.

5.2 The C-terminus domain is essential for the function of Gsdm/GSDM proteins

Each member of the *Gsdm* family, except for *GSDMB*, shows a characteristic expression pattern in epithelial tissue. *GsdmA/GSDMA* is expressed in the stratified squamous epithelium from skin to stomach. *GsdmC/GSDMC* and *GsdmD/GSDMD* are expressed in the gastrointestinal epithelium. In human, *GSDMB* is expressed in many kinds of tumor tissues and cancer cells (data unpublished). *GSDMA* and *GSDMB* are mapped to human chromosome 17q21, and *GSDMC* and *GSDMD* are mapped to 8q24, these two gene clusters reside in the vicinity of amplicon, which is frequently amplified in tumor cells (Bieche, *et al.*, 1996; Feo, *et al.*, 1996). This fact also supports that the common function of *Gsdm/GSDM* family is related to regulation of proliferation and differentiation of epithelial cells.

It was reported that *GSDMC/MLZE*, which is expressed in human melanoma, has a leucine-zipper motif (Watabe, *et al.*, 2001). However, it appeared in the separate

study of our group that this motif is not conserved among the *Gsdm/GSDM* family, but the motif found in the N-terminus and the unique leucine-rich C-terminus domain are highly conserved in the all family members. Besides *Rim3* and *Re^{den}*, in this study I identified a third mutation in *GsdmA-3*. This mutation *M00745* has a single base substitution, T1408A, which leads to nonsense mutation, Tyr442Stop. The tyrosine was included in the triplet amino acid sequence A-L-Y, which is conserved among all of the *Gsdm/GSDM* family (Figure 2C). In the *Rim3* mutation, the conserved Alanine is changed to Threonine (Ala348Thr). In the *Re^{den}* mutation, the length of interval of two conserved leucine residues, Leu399 and Leu413, is expanded by apposition of the two amino acids Glu-Ala. Thus, all three mutations occurred in the leucine-rich C-terminus domain of *GsdmA-3*. This fact suggests that the conserved C-terminus domain has essential role in the function of the *Gsdm/GSDM* family, possibly in regulation of proliferation and differentiation of epithelial cells.

5.3 *GsdmA-3* regulates differentiation of sebaceous glands and meibomian glands

In this study, I couldn't distinguish the expression pattern of *GsdmA-3* from that of *GsdmA-1* by *in situ* hybridization and immunohistochemistry, because of cross-hybridization of the cRNA probes and antibodies. The expression pattern of the *GsdmA-3* protein was, however, inferred from the immunohistochemical analysis with human and mouse skins. As mentioned earlier in this thesis, there are two related genes, *GsdmA-1* and *GsdmA-3*, in mouse genome, but there is only one gene *GSDMA* in the human genome. The amino acid sequence of the mouse *GsdmA-1* is much closer to that

of human GSDMA than to the mouse GsdmA-3. I found that the anti-mouse GsdmA-1(37) antibody produced in this study reacts with both mouse and human samples, but the same antibody gives strong signals for mouse sebocytes in sebaceous gland, but not for human sebocytes. All these data suggest that GsdmA-3, but not GsdmA-1, is expressed in mouse sebocytes.

I found that *Rim3/+* mice have abnormal meibomian gland. The meibomian gland is secretory organ in eyelids, as is the sebaceous glands associated with hair follicle. It is holocrine gland and secretes contents by burst of the terminally differentiated cells. Developmental origin of meibomian gland, however, is different from sebaceous gland. The progenitor cells of meibomian gland have different lineage from bulge stem cells (Olami, *et al.*, 2001). Notably, the phenotype of meibomian glands was different between *Rim3/+* and *M00745/+* mutant mice, although both mutations affect the sebaceous gland associated with hair follicles. The *M00745/+* mice possess sebocytes in the meibomian glands, but showed abnormal differentiation such as formation of ectopic hair-like structure and hyperplasia of the ductal epithelium. On the other hand, in *Rim3/+* mice the meibomian glands are cystic and hyperplastic, and no sebocytes were observed. Both *Rim3/+* and *Re^{den}/+* mice exhibited corneal opacity at 3 months of age (Sato *et al.*, 1998), but not *M00745/+* mice. The phenotype of the meibomian glands in *Rim3/+* mutants is much more severe than that of the *M00745/+* mice. The difference of these phenotypes may be attributable to the difference of the mutation-types of *GsdmA-3*. The results suggested that the conserved C-terminus and/or A-L-Y sequence have a function to regulate sebocyte differentiation,

regardless of cell lineage of the sebocytes.

5.4 *GsdmA-3* is involved in suppression of skin tumors development

This study clearly showed that the double heterozygotes of *Rim3* and *Trp53*⁻ mutations developed multiple skin tumors. Thus, the mice represent a new animal model of spontaneous squamous cell carcinoma (SCC). The *GsdmA-3* and *GSDMA* proteins are absent in proliferating cells in basal layer and dermal papilla of mouse and human normal skins. I found that these proteins are completely diminished or downregulated in skin tumors of both mouse and human. All the results suggested that *GsdmA-3* and *GSDMA* play a key role in suppression of tumor development. This is supported by the data obtained from collaboration with Dr. H. Sasaki of National Institute of Cancer, Tokyo, that colony formation of gastric tumor cells was suppressed by transfection with the wild-type *GsdmA-3* and *GSDMA* genes, and that the suppression was significantly reduced by transfection with the *Rex^{den}*-type mutant *GSDMA* gene (paper submitted).

There are many lines of evidence that function of tumor suppressor genes is inactivated in tumors. For example, *PTEN/Pten*, as known tumor suppressor of prostate cancer (Nelson and Carducci, 2000), is frequently inactivated by methylation of the promoter (Goel, *et al.*, 2004). Loss of heterozygosity (LOH) of *PTEN/Pten* is also shown in hereditary cancer syndrome Cowden's disease (Trojan, *et al.*, 2001). In the skin of *Pten* deficient mice, hyperkeratosis and spontaneous tumors are observed (Suzuki, *et al.*, 2003), as is the case of *Rim3* and *Trp53*⁻ double heterozygous mutants. Methylation of the promoter might be one of mechanism by which the expression of

GsdmA-3 and *GSDMA* are downregulated in skin tumors, because it was found that *GSDMA* was frequently silenced by DNA methylation in human gastric cancers (unpublished data). LOH and the methylation of the *GsdmA-3/GSDMA* promoter remain to be tested in mouse and human skin tumors in future study.

5.5 Molecular function of *GsdmA-3* and other *GsdmA/GSDMA* proteins in regulation of proliferation and differentiation of epidermal cells

Although the expression of *GsdmA-1* was not distinguished from that of *GsdmA-3* in this study, at least either *GsdmA-1* or *GsdmA-3* is expressed in differentiated keratinocytes in supra basal layer, and both genes are not expressed in proliferating cells in basal layer of interfollicular epidermis and upper follicular epidermis, as well as neoplastic cells. Then, it is puzzling that *GsdmA-3* expressing cells are physically distant from basal cell layer, which is affected in the *GsdmA-3* mutations. One may interpret this by a model as shown in Figure 22. In this model, differentiated cells in supra basal layer may have an activity to suppress proliferation of differentiated cells and stem cells in basal layer by either direct cellular interaction or secreted signal(s). In epidermis of *GsdmA-3* mutants, the differentiated cells possibly lose the suppressive activity. This model is supported by following facts: i) Transfection with wild-type *GsdmA-3* and human *GSDMA* genes suppresses proliferation of human gastric tumor cells, but the *Rex^{den}*-type mutant human *GSDMA* gene showed reduced suppression activity. Thus, the *GsdmA-3* mutation likely decreases or loses the suppressive activity of the *GsdmA-3* and *GSDMA* genes. ii) It was reported that differentiated cells in supra

basal layer negatively regulates proliferation of basal stem cells. For instance, conversion of carcinogen-induced papilloma to malignant SCC is less frequently observed in transgenic mice, in which $\alpha 3\beta 1$ integrin is overexpressed in the supra basal layer of epidermis, than in wild-type mice (Owens, *et al.*, 2001). It was also reported that in the olfactory epithelium, differentiated neurons produce growth and differentiation factor 11 (Gdf11), which inhibit proliferation of precursor cells as a feed back system (Wu *et al.*, 2003). Taken together, the model is most likely mechanism by which physically distant differentiated cells in supra basal layer regulate proliferative stem cells in basal cell layer.

At present, it is unclear why the *GsdmA-3* mutants show unidirectional migration of stem cells. The hyperproliferation was initially observed in the interfollicular and the upper follicular epidermis in *Rim3/+* mice (data not shown). Therefore, it is likely that *GsdmA-3* is predominantly expressed in interfollicular and upper follicular epidermis, and the function of the *GsdmA-3* may regulate proliferation and differentiation of stem cells in the bulge region.

Immunoelectron microscopic observation in this study indicated that *GsdmA-1/GsdmA-3* proteins are localized in cytoplasm and plasma membrane, and localization of the proteins in undefined vesicles was also observed. The results may imply that the function of the *GsdmA* proteins is correlated to the signal transduction from plasma membrane. It was reported that absence of *Caveolin-1*, a principal component of caveolar membrane coat, increases susceptibility to epidermal hyperplasia and skin tumor by oncogenic stimulus (Capozza, *et al.*, 2003). In other reports, Connexin 26

(Cx26), which acts to form gap junction, is expressed in suprabasal layer. In human, mutation of *Cx26* is found in the true Vohwinkel syndrome (VS) (Maestrini, *et al.*, 1999), which is characterized by the hyperproliferation of the epidermis of palms and soles (Vohwinkel, 1929). Targeted epidermal expression of mutant-type *Cx26* in suprabasal layer mimics the VS (Bakirtzis, *et al.*, 2003). Moreover, it is known that localization of Cx26 is shifted from intercellular junction to cytoplasm in the case of VS. Likewise, the localization pattern of GsdmA proteins differs in *Rim3/+* and the wild-type mice. The proteins are accumulated in the cytoplasm in the spinous and the granular layers in the *Rim3/+* mice, but not in wild-type mice. It was also observed in this study that localization pattern of GsdmA-1 and GsdmA-3 proteins coincide with the staining pattern of the nuclear by HE. It is possible that the change of intra-cellular localization of the GsdmA proteins modulates their function related to proliferation and differentiation of epidermal cells. The GsdmA proteins localized in plasma membrane may act to downregulate cell proliferation. The proteins localized in the cytoplasm may facilitate terminal differentiation.

Another possible mechanism by which the GsdmA proteins suppress the proliferation of basal stem cells may be employed as secreted factors. Terminal differentiating keratinocytes produce transforming growth factor- β (Tgf- β), which is known to inhibit epidermal proliferation (Akhurst, *et al.*, 1988). In human, GSDMA is also localized in intra-ductal component of eccrine sweat glands (Figure 18D and 18E). Like exocrine glands, eccrine sweat glands secrete sweat including growth factor such as interleukin-1 α (IL-1) (Sato and Sato, 1994) and epidermal growth factor (EGF) (Saga

and Jimbow, *et al.*, 2001). As GsdmA proteins are localized in plasma membrane and/or undefined vesicles/organelles, GSDMA proteins are possibly secreted through cell membranes, and act as a negative regulator for cell proliferation.

6. Acknowledgements

I wish to express my sincere gratitude to my supervisor, Prof. Toshihiko Shiroishi, for his advice and stimulating discussion. I particularly appreciate Dr. Masaru Tamura for his exciting discussion and technical advice throughout this study. I also appreciate Dr. Hiroki Sasaki for invaluable data on *GSDMA* and informative advice. I also thank Drs. Shigeharu Wakana and Hiroshi Masuya for *M00745* mutant generated by ENU mutagenesis. I also grateful to Dr. Kyoji Hioki for *Trp53* knockout mice. I greatly appreciate Mrs. Keiko Hiratsuka, Katsue Aida, Michiko Arie, Fumie Murofushi, Mr. Akiteru Maeno and other staffs of animal facility of the National Institute of Genetics for taking care of the mice used in this study. I also thank Mr. Yoichi Mizushina, Mrs. Noriko Yamatani and Miss. Hiromi Yamamoto for supplying *Rim3* and *Re^{den}* mutant mice by manipulating the embryos of the mice. I am also grateful to Drs. Hiroaki Yamamoto, Kiyokazu Morioka and Hidenori Suzuki for reviewing the histology of immunoelectron microscopy and for valuable advice for this study. I thank Drs. Ryo Wada, Hideaki Toki and Satoshi Nishikawa for reviewing the histology of skin tumors. I also thank Dr. Aya Aoki, Mr. Tomoaki Fujii, Dr. Hiromitsu Komiyama, Mr. Ryu Kashiwagi and Mrs. Yoriko Kato and other members of Mammalian Genetics Laboratory for valuable suggestions and supporting this work.

7. References

Akhurst, R. J., Fee, F. and Balmain, A. Localized production of TGF-beta mRNA in tumour promoter-stimulated mouse epidermis. *Nature*, 331, 363-365, 1988.

Bakirtzis, G., Choudhry, R., Aasen, T., Shore, L., Brown, K., Bryson, S., Forrow, S., Tetley, L., Finbow, M., Greenhalgh, D. and Hodgins, M. Targeted epidermal expression of mutant Connexin 26(D66H) mimics true Vohwinkel syndrome and provides a model for the pathogenesis of dominant connexin disorders. *Hum. Mol. Genet.*, 15, 1737-1744, 2003.

Bieche, I., Tomasetto, C., Regnier, C. H., Moog-Lutz, C., Rio, M. C. and Lidereau, R. Two distinct amplified regions at 17q11-q21 involved in human primary breast cancer. *Cancer Res.*, 56, 3886-3890, 1996.

Capozza, F., Williams, T. M., Schubert, W., McClain, S., Bouzahzah, B., Sotgia, F. and Lisanti, M. P. Absence of caveolin-1 sensitizes mouse skin to carcinogen-induced epidermal hyperplasia and tumor formation. *Am. J. Pathol.*, 162, 2029-2039, 2003.

Cotsarelis, G., Sun, T. T., and Lavker, R.M. Label-retaining bromodeoxyuridine incorporation cells reside in the bulge area of pilosebaceous unit: implications for follicular stem cells, hair cycle, and skin carcinogenesis. *Cell*, 61, 1329 -1337, 1990.

Cotsarelis, G., Kaur, P., Dhouailly, D., Hengge, U., and Bickenbach, J. Epithelial stem cells in the skin: definition, markers, localization and functions. *Exp. Dermatol.*, 8, 80-88, 1999.

DasGupta, R., Rhee, H. and Fuchs, E. A developmental conundrum: a stabilized form of beta-catenin lacking the transcriptional activation domain triggers features of hair cell fate in epidermal cells and epidermal cell fate in hair follicle cells. *J. Cell Biol.*, 158, 331-344, 2002.

Delfino, V., Casartelli, G., Garzoglio, B., Scala, M., Mereu, P., Bonatti, S., Margarino, G. and Abbondandolo, A. Micronuclei and p53 accumulation in preneoplastic and malignant lesions of the head and neck. *Mutagenesis*, 17, 73-77, 2002.

Donehower, L. A., Harvey, M., Slagle, B. L., McArthur, M. J., Montgomery Jr, C. A., Butel, J. S. and Bradley, A. Mice deficient for p53 are developmentally normal but susceptible to spontaneous tumours. *Nature*, 356, 215-221, 1992.

Feo, S., Di Liegro, C., Mangano, R., Read, M. and Fried, M. The amplicons in HL60 cells contain novel cellular sequences linked to MYC locus DNA. *Oncogene*, 13, 1521-1529, 1996.

Fuchs, E., and Segre, J. A. Stem cells: a new lease on life. *Cell*, 100, 143-155, 2000.

Gat, U., DasGupta, R., Degenstein, L. and Fuchs, E. De novo hair follicle morphogenesis and hair tumors in mice expressing a truncated beta-catenin in Skin. *Cell*, 95, 605-614, 1998.

Giglia-Mari, G. and Sarasin, A. *TP53* mutations in skin cancers. *Hum. Mutat.*, 21, 217-228, 2003.

Goel, A., Arnold, C. N., Niedzwiecki, D., Carethers, J. M., Dowell, J. M., Wasserman, L., Compton, C., Mayer, R. J., Bertagnolli, M. M. and Boland, C. R. Frequent Inactivation of PTEN by Promoter Hypermethylation in Microsatellite Instability-High Sporadic Colorectal Cancers. *Cancer Res.*, 64, 3014-3021, 2004

Grachtchouk¹, M., Mo, R., Yu, S., Zhang, X., Sasaki, H., Hui, C. C. and Dlugosz¹, A. A. Bacal cell carcinomas in mice overexpressing *Gli2* in skin. *Nat. Genet.* 24, 216-217, 2000.

Hardy, M. H. The secret life of the hair follicle. *Trends Genet.*, 8, 159-166, 1992.

Huelsken, J., Vogel, R., Erdmann, B., Cotsarelis, G. and Birchmeier W. Beta-catenin controls hair follicle morphogenesis and stem cell differentiation in the skin. *Cell*, 105, 533-545, 2001.

Jonason, A. S., Kunala, S., Price, G. J., Restifo, R. J., Spinelli, H. M., Persing, J. A., Leffell, D. J., Tarone, R. E. and Brash, D. E. Frequent clones of p53-mutated keratinocytes in normal human skin. *Proc. Natl. Acad. Sci. U S A*, 93, 14025-14029, 1996.

Kiguchi, K., Bol, D., Carbajal, S., Beltran, L., Moats, S., Chan, K., Jorcano, J. and DiGiovanni, J. Constitutive expression of erbB2 in epidermis of transgenic mice results in epidermal hyperproliferation and spontaneous skin tumor development. *Oncogene*, 19, 4243-4254, 2000.

Kokkola A., Monni O., Puolakkainen P., Larramendy ML, Victorzon M., Nordling S., Haapiainen R., Kivilaakso E. and Knuutila S. 17q12-21 amplicon, a novel recurrent genetic change in intestinal type of gastric carcinoma: a comparative genomic hybridization study. *Genes Chromosomes Cancer.*, 20, 38-43, 1997.

Lavker, R. M., and Sun, T. T. Epidermal stem cells: properties, markers, and location. *Proc. Natl. Acad. Sci. USA.* 97, 13473-13475, 2000.

Li, Q. L., Ito, K., Sakakura, C., Fukamachi, H., Inoue, K., Chi, X. Z., Lee, K. Y., Nomura, S., Lee, C. W., Han, S. B., Kim, H. M., Kim, W. J., Yamamoto, H., Yamashita, N., Yano, T., Ikeda, T., Itohara, S., Inazawa, J., Abe, T., Hagiwara, A., Yamagishi, H.,

Ooe, A., Kaneda, A., Sugimura, T., Ushijima, T., Bae, S. C. and Ito, Y. Causal relationship between the loss of RUNX3 expression and gastric cancer. *Cell*. 109, 113-124, 2002.

Owens, D. M. and Watt, F. M. Influence of $\beta 1$ integrins on epidermal squamous cell carcinoma formation in a transgenic mouse model: $\alpha 3\beta 1$, but not $\alpha 2\beta 1$, suppresses malignant conversion. *Cancer Res.*, 61, 5248-5245, 2001.

Maestrini, E., Korge, B. P., Ocana-Sierra, J., Calzolari, E., Cambiaghi, S., Scudder, P. M., Hovnanian, A., Monaco, A. P. and Munro, C. S. A missense mutation in connexin26, D66H, causes mutilating keratoderma with sensorineural deafness (Vohwinkel's syndrome) in three unrelated families. *Hum. Mol. Genet.*, 8, 1237-1243, 1999.

Mansbridge, J. and Knapp, A. M. Changes in keratinocyte maturation during wound healing. *J. Invest. Dermatol.*, 89, 253-263, 1987.

Merajver, S. D., Pham, T. M., Caduff, R. F., Chen, M., Poy, E. L., Cooney, K. A., Weber, B. L., Collins, F. S., Johnston, C. and Frank, T. S. Somatic mutations in the BRCA1 gene in sporadic ovarian tumours. *Nat. Genet.*, 4, 439-443, 1995.

Merrill, B. J., Gat, U., DasGupta, R. and Fuchs, E. Tcf3 and Lef1 regulate lineage differentiation of multipotent stem cells in skin. *Genes Dev.*, 15, 1688-1705, 2001.

Muller-Rover, S., Handjiski, B., Van Der Veen, C., Eichmuller, S., Foitzik, K., McKay, I. A., Stenn, K. S. and Paus, R. A comprehensive guide for the accurate classification of murine hair follicles in distinct hair cycle stages. *J. Invest. Dermatol.*, 117, 4-15, 2001.

Nelson, J. B. and Carducci, M. A. Small bioactive peptides and cell surface peptidases in androgen-independent prostate cancer. *Cancer Invest.* 18, 87-96, 2000.

Niemann, C., Owens, D. M., Hulsken, J., Birchmeier, W. and Watt, F. M. Expression of delta-N Lef1 in mouse epidermis results in differentiation of hair follicles into squamous epidermal cysts and formation of skin tumors. *Development*, 129, 95-109, 2002.

Olami, Y., Zajicek, G., Cogan, M., Gnessin, H. and Pe'er, J. Turnover and migration of meibomian gland cells in rat's eyelids. *Ophthalmic Res.*, 33, 170-175, 2001

Oshima, H., Rochat, A., Kedzia, C., Kobayashi, K. and Barrandon, Y. Morphogenesis and renewal of hair follicles from adult multipotent stem cells. *Cell*, 104, 233-245, 2001.

Paus, R., Muller-Rover, S., Van Der Veen, C., Maurer, M., Eichmuller, S., Ling, G., Hofmann, U., Foitzik, K., Mecklenburg, L. and Handjiski, B. A comprehensive guide

for the recognition and classification of distinct stages of hair follicle morphogenesis. *J. Invest. Dermatol.*, 113, 523-532, 1999.

Saeki, N., Kuwahara, Y., Sasaki, H., Sato, H. and Shiroishi, T. Gasdermin (*Gsdm*) localizing to mouse Chromosome 11 is predominantly expressed in upper gastrointestinal tract but significantly suppressed in human gastric cancer cells. *Mammal. Genome*, 11, 718-724, 2000.

Saga, K. and Jimbow, K. Immunohistochemical localization of activated EGF receptor in human eccrine and apocrine sweat glands. *J. Histochem. Cytochem.*, 49, 597-602, 2001.

Sato, K. and Sato, F. Interleukin-1 alpha in human sweat is functionally active and derived from the eccrine sweat gland. *Am. J. Physiol.*, 266, R950-959, 1994.

Sato, H., Koide, T., Masuya, H., Wakana, S., Sagai, T., Umezawa, A., Ishiguro, S., Tamai, M. and Shiroishi, T. A new mutation *Rim3* resembling *Re^{den}* is mapped close to retinoic acid receptor alpha (*Rara*) gene on mouse chromosome 11. *Mammal. Genome*, 9, 20-25, 1998.

Stein, D., Wu, J., Fuqua, S. A., Roonprapunt, C., Yajnik, V., D'Eustachio, P., Moskow, J. J., Buchberg, A. M., Osborne, C. K. and Margolis, B. The SH2 domain protein GRB-7

is co-amplified, overexpressed and in a tight complex with HER2 in breast cancer.

EMBO J., 13, 1331-1340, 1994.

Suzuki, A., Itami, S., Ohisi, M., Hamada, K., Inoue, T., Komazawa, N., Senoo, H., Sasaki, T., Takeda, J., Manabe, M., Mak, T. W. and Nakano, T. Keratinocyte-specific Pten deficiency results in epidermal hyperplasia, accelerated hair follicle morphogenesis and tumor formation. *Cancer Res.*, 63, 674-681, 2003.

Tiffany, J. M., The role of meibomian secretion in the tears. *Trans. Ophthalmol. Soc. UK*, 104, 396-401, 1985

Trojan, J., Plotz, G., Brieger, A., Raedle, J., Meltzer, S. J., Wolter, M. and Zeuzem, S. Activation of a cryptic splice site of PTEN and loss of heterozygosity in benign skin lesions in Cowden disease. *J. Invest. Dermatol.*, 117, 1650-1653, 2001.

Tsukada, T., Tomooka, Y., Takai, S., Ueda, Y., Nishikawa, S., Yagi, T., Tokunaga, T., Takeda, N., Suda, Y., Abe, S., Matsuo, I., Ikawa, Y. and Aizawa, S. Enhanced proliferative potential in culture of cells from p53-deficient mice. *Oncogene*, 8, 3313-3322, 1993.

Vohwinkel, H. Keratoderma hereditaria mutilans. *Arch. Dermatol. Syphilol.*, 158, 354-364, 1929.

Watabe, K., Ito, A., Asada, H., Endo, Y., Kobayashi, T., Nakamoto, K., Itami, S., Takao, S., Shinomura, Y., Aikou, T., Yoshikawa, K., Matsuzawa, Y., Kitamura, Y. and Nojima, H. Structure, expression and chromosome mapping of MLZE, a novel gene which is preferentially expressed in metastatic melanoma cells. *Jpn. J. Cancer Res.*, 92, 140-151. 2001.

Watt, F. M., and Hogan, B. L. Out of Eden: stem cells and their niches. *Science*, 287, 1427-1430, 2000.

Wu, H. H., Ivkovic, S., Murray, R. C., Jaramillo, S., Lyons, K. M., Johnson, J. E. and Calof, A. L. Autoregulation of neurogenesis by GDF11. *Neuron*, 197-207, 2003.

Wu, X. and Pandolfi, P. P. Mouse models for multistep tumorigenesis. *Trends cell Biol.*, 11, S2-S9, 2001.

Xie, W., Chow, L. T., Paterson, A. J., Chin, E. and Kudlow, J. E. Conditional expression of the *ErbB2* oncogene elicits reversible hyperplasia in stratified epithelia and up-regulation of *TGFalpha* expression in transgenic mice. *Oncogene*, 18, 3593-3607, 1999.

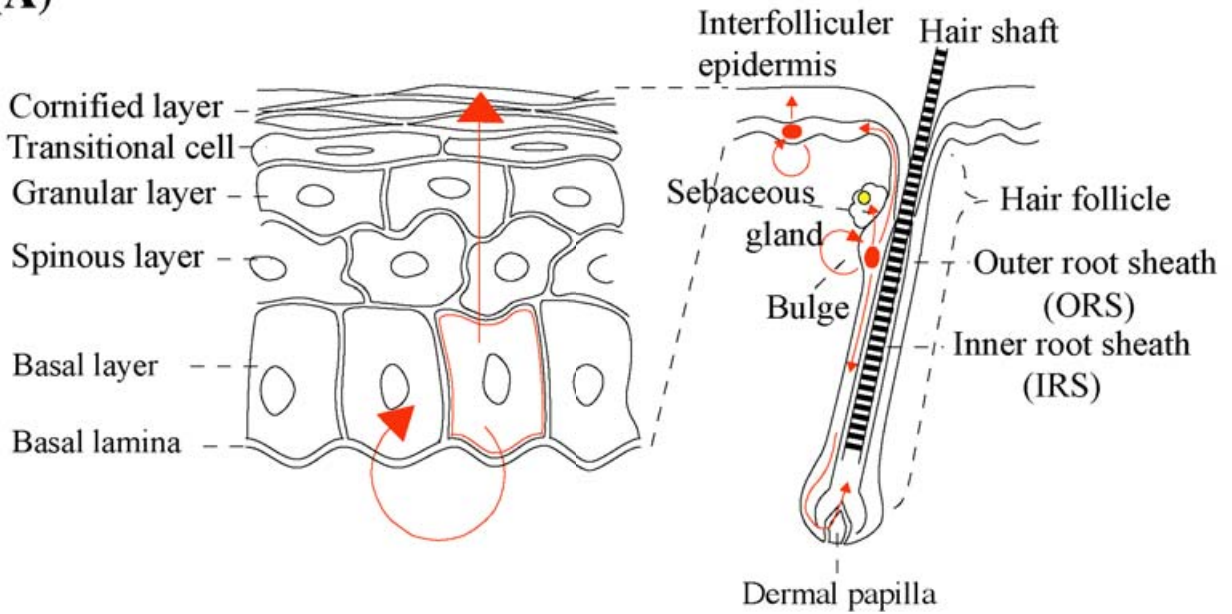
Table 1. Incidence of spontaneous skin tumors in the progeny generated from the cross of the *Rim3*^{+/+} and *Trp53*^{-/+} mice

Genotype		Number of mice observed	Number of mice with skin tumors	Number of skin tumors	Number of mice (%)				
<i>GsdmA-3</i>	<i>Trp53</i>				Head	Neck	Trunk	Buttock	Other
+/+	+/+	21	0	0	—	—	—	—	—
+/+	-/+	20	0	0	—	—	—	—	—
<i>Rim3</i> ^{+/+}	+/+	19	2	2	—	—	2 (100)	—	—
<i>Rim3</i> ^{+/+}	-/+	21	17	36	11 (31)	16 (44)	6 (16)	1 (3)	2 (6)

Figure 1. Diagram of epidermal stem cells and hair cycle. (A) Location and migration of epidermal stem cells. Epidermal stem cells reside in both basal layer and bulge of hair follicles. While the stem cells in basal layer differentiate into epidermal keratinocytes, those in bulge give rise to not only hair follicles but also interfollicular epidermis and sebaceous glands. (B) Morphological change of hair follicle during hair cycle. In postnatal stage, hair follicles periodically exhibit growth and regression. Dermal papilla grows toward to dermis in deep and hair shaft also grows from the dermal papilla in the anagen phase. In the phase known as catagen, lower hair follicles are degenerated by apoptosis. This draws the dermal papilla up to the bulge region (broken line). Following this resting period known as telogen, hair shaft stops the growth and comes off.

Figure 1

(A)



(B)

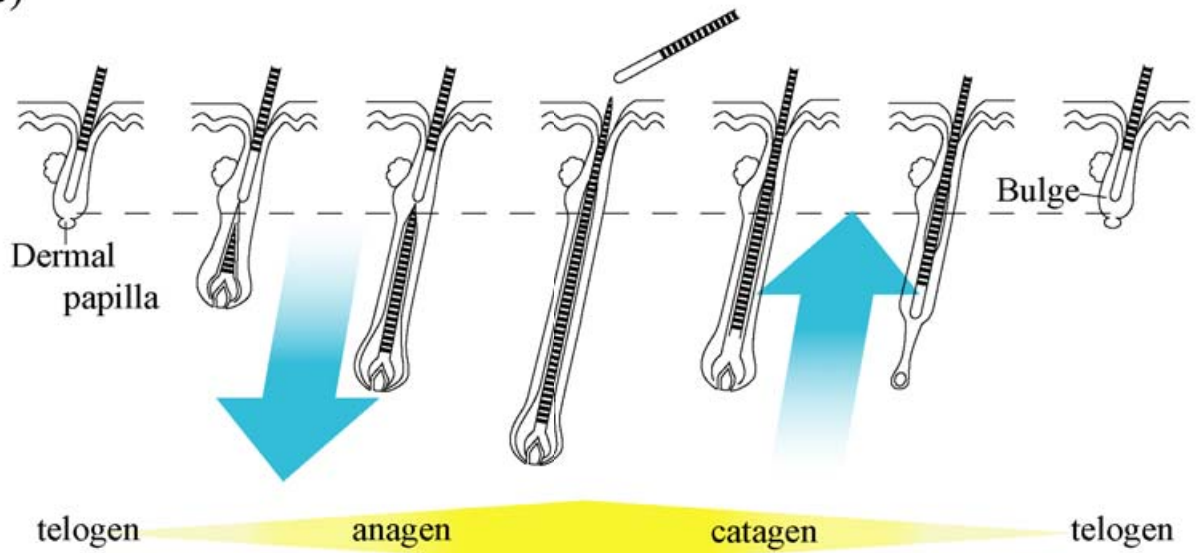


Figure 2. Genomic structure of the *GsdmA/GSDMA* genes and phylogenetic tree of *Gsdm/GSDM* gene family. (A) Genomic structure of *GsdmA/GSDMA* genes. (B) Phylogenetic tree of the *Gsdm/GSDM* gene family. The tree was constructed by the NJ method. Multiple amino acid sequences were aligned using CLUSTALW (<http://www.ddbj.nig.ac.jp>). (C) Sequence alignment of the *Gsdm* gene family. Magenta boxes 1 and 2 indicate antigen peptides used for production of anti-GsdmA antibodies: box1(37CLVLRKRKSTLF) is common among GsdmA-1, GsdmA-2, GsdmA-3 and GSDMA and used for production of anti-GsdmA antibody; box2 (246QMISEEPEEEKLG) is specific to GsdmA-3 and used for production of anti-GsdmA-3 antibody. Green boxes 1, 2 and 3 indicate positions of the *Rim3*, *Re^{den}* and *M00745* mutations, respectively. The identical amino acid residues through all the family members are asterisked below the alignment. A colon and a period indicate substitutions with highly conserved and less conserved residues, respectively.

(2/2)

Mouse GsdmA-1	LAYRVRQLMVNGKDEWGIPIHCND-----SMQTFPPGE	236
Mouse GsdmA-2IIY.....Y..T-----N.P..N.--	254
Mouse GsdmA-3L.R.FLNL.D..Y.....KIR	236
Human GSDMA	..F.....K.....D-----N.....	235
Mouse GsdmC-1	...KKQ..VIEDNTCVILT-----AN.KKKMT	234
Mouse GsdmC-2	...KKQ..VIENNTCVIL-----ATKKKMTF	231
Mouse GsdmC-3	...KKQ..VIENNTCVIL-----ATKKKMTF	231
Human GSDMC	M..KRK..VIKE.AILISDDDEQRTFQDEYEISEMVGYCAARSEGLLPSFHTISPTLFNA	272
Mouse GsdmD	..F..A..LIG--SK.D.LLVSDE-----KQR..E.SS	245
Human GSDMD	..F..A..VID--SDLDVLLFPDK-----KQR..Q.PA	244
Human GSDMB	..S...K..VFPN.ETMN.HFRGKT-----KS..EEK	235
	:::: * .	
Mouse GsdmA-1	KPGEKFIL-----IQASDVGEMHEDFKTLKEEVQRETQVEVK	274
Mouse GsdmA-2	LCVLQRQGS-----TVQMIS.....K...Q.....	292
Mouse GsdmA-3	RVPCSA..SPTQM-----ISEEPEEEKLI..	283
Human GSDMA	..S..E.V.....D.V..G.R.....Q...	273
Mouse GsdmC-1	--FPMR.VGMSGHLRYQDLVIETGSWINDIDPIGTIKEPT.L..MC.QN..SEQ.RLLAE	292
Mouse GsdmC-2	PDRPL.LYDLPVTLRYQEVIETGSWIDDIDPIGTIEBPANLN.MC.QH..SEQ..LLAE	291
Mouse GsdmC-3	PGTPKYASASEPTEIYRTELQG--LWINDIVPIGRIQEPA.L..MC.QN..YKQ.EQLAE	289
Human GSDMC	SSNDM.LKPELFLTQQPLSGHLPKYEQVHILPVGRIEPPFQWQ..H.Q...FQIKITLQA	332
Mouse GsdmD	GDRKAVGQRHHGLNVLAALCSIGKQLSLLSDGIDEEBLIEAA..QG.YA..KACSS.L.S	305
Human GSDMD	TGHRKSTSEGAWPQLPSGLSMRCLHNFLTGDGVP-AE.AFT...QG.RA..ETISK.L.L	303
Human GSDMB	DGASSCLG-----KSLGS..SRNM..KLEDMESVLKD	267
	. : : :	
Mouse GsdmA-1	LSPVGRSLLTSLSHLLG--KKKELQDLEQTLLEGALDKGHEVTLEALPKDVLLSKDAMD-	331
Mouse GsdmA-2M.....P.....L.....	349
Mouse GsdmA-3K.....QK.....	340
Human GSDMA	..R..Q...S...K.....LA.....E.VG-	330
Mouse GsdmC-1	..KDVQEVVFS.FL.M.C--DRDV.Y..MKM..LNQLGH----MDG.GGKI.DELRK.S	345
Mouse GsdmC-2	..KDVQEVVFS.FL.M.S--DRDV.Y..MKM..LNQLGH----MDG.GGKI.DELRK.S	344
Mouse GsdmC-3	..KGVQEVV.S.ILSM.YEGDR.V.Y..MNM..LNQLGH----MDG.GGKI.DELRK.S	344
Human GSDMC	..KDVQDVVMFY.ILAM.R--DRGA...MNM..LDSSGH----LDG.GGAI.K.LQQ.S	385
Mouse GsdmD	.EMEL.QQI.VNIGKI.Q--DQPSMEA..AS.GQG.CS.GQ.EPLDG.AGCI.ECLVL.S	363
Human GSDMD	.DRELCQL..EG.EGV.R--DQLA.RA..EA..QGQSL.-P.EPLDG.AGAV.ECLVLSS	360
Human GSDMB	.TEEK.KDV.N..AKC...EDIR...RVSEV.IS--ELHMED.DKP..SLFNAA	323
	* . : : * .. * : * : *	
Mouse GsdmA-1	-----AILYFLGALTVLSEAQQKLLVKSLEKKILPVQLKLVESTMEKNFLQDKEGV	382
Mouse GsdmA-2E..E.L.I.....N.V.....IL.Q.....D.	400
Mouse GsdmA-3E.T.E.L.I.....L.Q.....	391
Human GSDMAV.....E.....M.....Q...L....	381
Mouse GsdmC-1	SLSWINLKDL..L.Q..M..DT.LC..AL.V.MRL..H.VE..K.ILQP..KYPWNIP	405
Mouse GsdmC-2	STPHDVLKDLN..L.Q..L..DT.LC..AQ.VKMGL..H.VE..K.ILQT..KYSSNTP	404
Mouse GsdmC-3	SNPCVDLKDL..L.Q..M..DS.LN..AQ.V.MG..H.VE..K.ILQP..KYPWNIP	404
Human GSDMC	NHAWFNPKDP..L.E.IM..DF.HD..AC.M..R..LQ.QE..R.I.L.P..RYPWSIP	445
Mouse GsdmD	GELVPELAAP.F.L...A...T..Q..A.A..TTV.SK..E..KHVL.QSTPWQEQSS	423
Human GSDMD	GMLVPELAIPVV.L...M..T.H...AEA..SQT.LGP.E..G.LL.QSAPWQERST	420
Human GSDMB	GVLVEARAK...D..D..LE...E.QFVAEA...GT..LLKDQ.K.V..Q.WD-----	376
	. : : * : * : : : : * . * : : .	
Mouse GsdmA-1	FPLQPDLLSSSLGEEELILTEALVGLSGLEVQRSGPQYTWDPTLPHLCALYAGLSLLQLL	442
Mouse GsdmA-2	...R.....DQ.....N...CHN.....H..	460
Mouse GsdmA-3T..E.....A.....RHN.....H..	451
Human GSDMA	...E.....D...T.....M.....R.....Q.	441
Mouse GsdmC-1	.T...Q..AP.QG.G.AI.YE.LEEC..KMELNN.RS..LEAKMP.S...GS..F..Q.	465
Mouse GsdmC-2	.T...Q..AP.QG.G.AI.YE.LEEC..KMELNN.RS..LEAKMP.S...GS..F..Q.	464
Mouse GsdmC-3	.T...Q..AP.QG.G.AI.YE.LEEC..KMELNN.RS..LEAKMP.S...GS..F..Q.	464
Human GSDMC	.T.K.E..AP.QS.G.AI.YG.LEEC..RMELDN.RS..VEAKMP.S...GT....Q.	505
Mouse GsdmD	VS.PTV..GDCWD.K-NP.WV.LEEC..RL.VES..VH.E.TS....S.F..SS.	483
Human GSDMD	MS.P.G..GNSWG.G-APAWV.LDEC...LGEDT.HVC.E.QAQGRM....S.A..SG.	480
Human GSDMB	-----LAS.P.DMDY..EAR-I.....VVV.I.LE.	407
	. : . * : : : .*** : : * *	
Mouse GsdmA-1	SKNS-----	445
Mouse GsdmA-2	.RD-----	464
Mouse GsdmA-3	.RK.NALTYCALS---	464
Human GSDMA	T.A-----	445
Mouse GsdmC-1	.EA-----	468
Mouse GsdmC-2	Q.ANSSSKPSLSPGYI	480
Mouse GsdmC-3	R.ANSSSKPSLRPGYI	480
Human GSDMC	AEA-----	508
Mouse GsdmD	GQKPC-----	488
Human GSDMD	.QEPH-----	485
Human GSDMB	AEGPTSVSS-----	415

Figure 3. Analysis of expression patterns of *GsdmA-1* and *GsdmA-3* by RT-PCR. (A) Spatial expression patterns of *GsdmA-1* and *A-3*. *GsdmA-1* is expressed in skin and stomach, and *GsdmA-3* specifically in skin. *GsdmA-2* is expressed only in stomach (data not shown). (B) Analysis of temporal expression patterns of *GsdmA-1* and *A-3* in skin by RT-PCR. The expression of *GsdmA-1* starts at E15.5 and continues through all embryonic stages to postnatal stage. The expression of *GsdmA-3* starts from postnatal stage in skin.

Figure 4. Expression analysis of *GsdmA-1* and *GsdmA-3* by *in situ* hybridization. Sagittal cryosections of dorsal skin of 1 month-old wild-type (A, C, E and G) and *Rim3/+* (B, D, F and H) mice were hybridized with a cRNA probe that hybridize *GsdmA-1* and *GsdmA-3*. *GsdmA-1* and/or *GsdmA-3* are expressed in granular layer of interfollicular epidermis in wild-type and *Rim3* mice (arrows in A, B, C and D), and are intensely expressed in sebaceous glands in wild type (white arrows in A and E). In hair follicles, they are expressed in the inner root sheath (IRS) in wild-type and *Rim3* mice (arrowheads in A, B, G and H), but are not expressed in the dermal papilla (dp) (G and H). In *Rim3/+* mice, no expression of the genes was observed in the sebaceous glands, because of abnormal morphology of the glands in *Rim3/+* (F). The broken line indicates basal lamina (C and D). Asterisks are melanin in the hair (A, C, D and H). Scale bar is 50 μm .

Figure 4

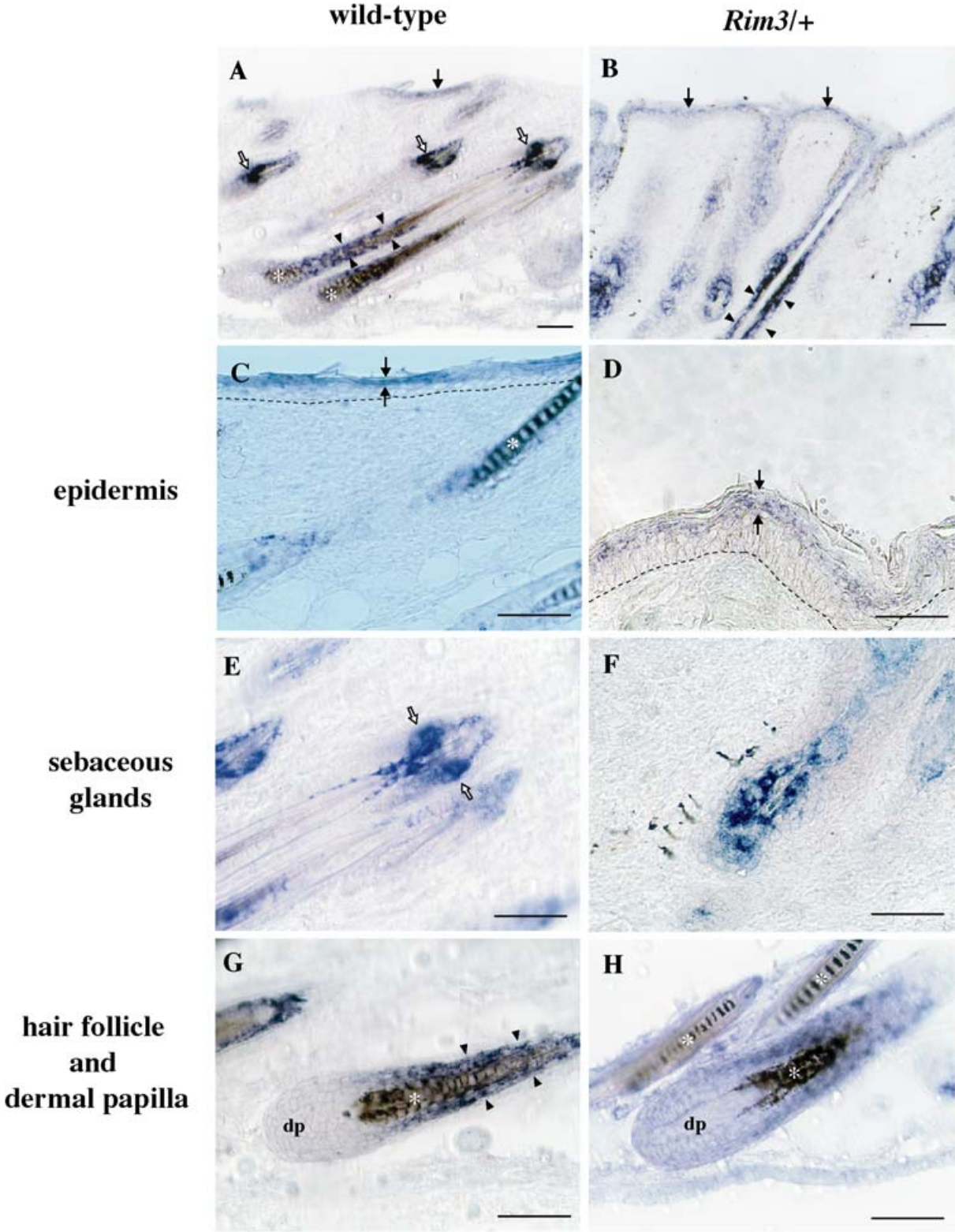


Figure 5. Time course of histological change of the hair follicles of *Rim3/+* mice. Sagittal sections of dorsal skin of 1 month-old (A and B), 3 months-old (D and E) and 10 months-old (G and H) wild-type and *Rim3/+* mice were stained with Hematoxylin and Eosin. The gross phenotype of 1 month- (C), 3 months- (F) and 10 months-old (I) *Rim3/+* mice. The developmental stages of the hair follicles are synchronized in wild-type mouse through the all ages (arrowheads in A, D and G). In 1 month-old *Rim3/+* mice, the dermal papillas were formed in different directions (arrowheads in B) and keratins were accumulated in the upper hair follicles (arrows in B). Anagen phase and abnormal catagen phase coexist in *Rim3/+* (arrowhead and asterisk in E). Finally, all hair follicles were completely lost in *Rim3/+* (H). Scale bar is 50 μm .

Figure 5

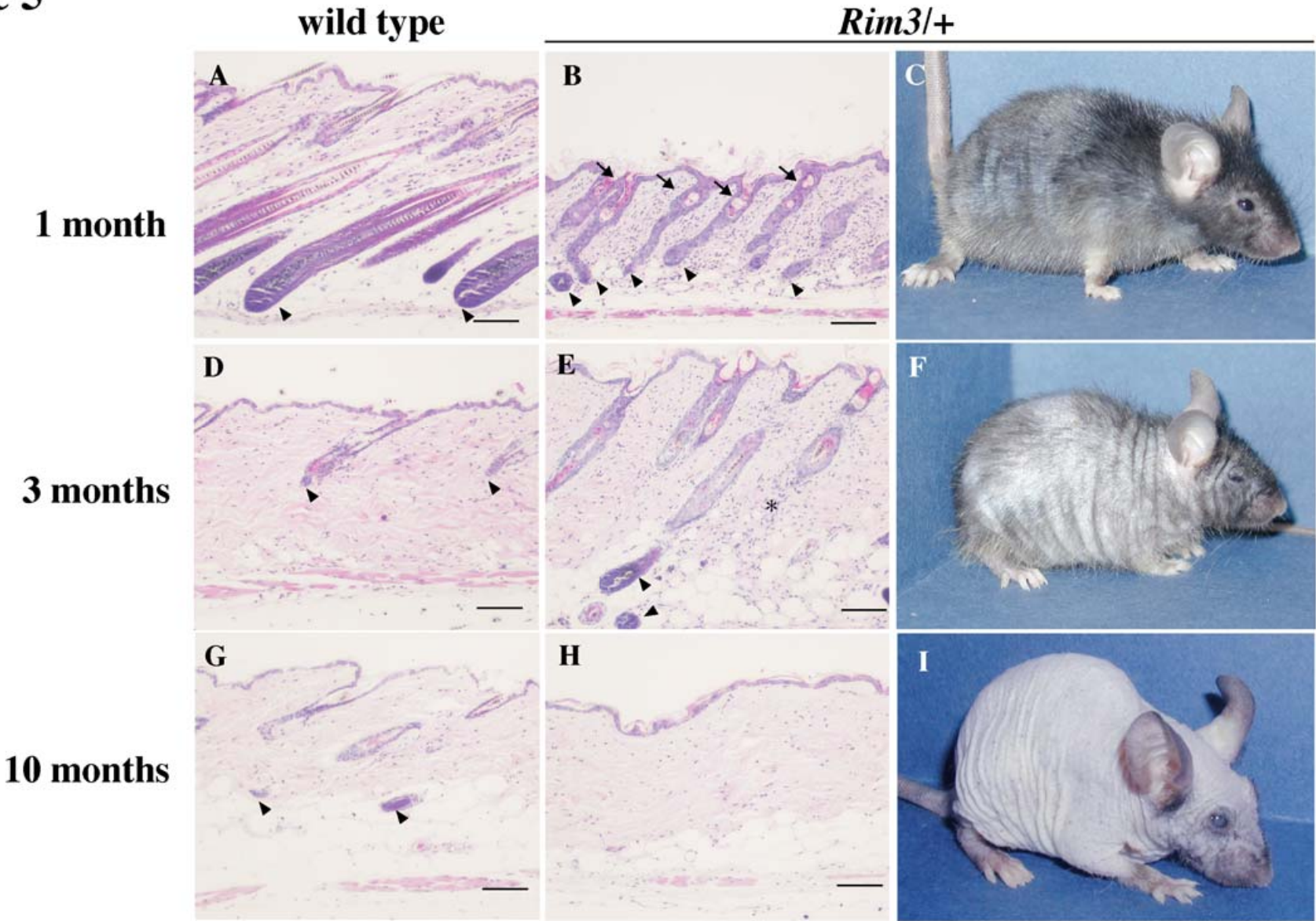


Figure 6. Immunohistochemical analysis of differentiation of the epidermis in *Rim3/+* mouse. Sagittal paraffin sections of dorsal skin of wild-type (A, C, E and G) and *Rim3/+* mouse (B, D, F and H) at 3 months of age were stained with anti-keratin antibodies. The green signal depicts the staining of the antibodies, and the red DAPI DNA staining (A-F). Staining with anti-K14 antibody (A and B), which recognizes basal layer and outer root sheath (ORS) in wild-type skins, revealed hyperplasia of epidermal and follicular cells in *Rim3/+* (arrows in A and B). Staining with anti-K10 antibody (C and D), which detects granular layer in the wild-type mouse and is an epidermis marker of terminal differentiation, showed ectopic expression in the upper hair follicles in *Rim3/+* (arrow in D). K6 is a marker of ORS and wounding epidermis in wild-type mouse (E). K6 was expressed in the hair follicles and the epidermis of *Rim3/+* (arrows in F). Scale bar is 50 μm .

Figure 6

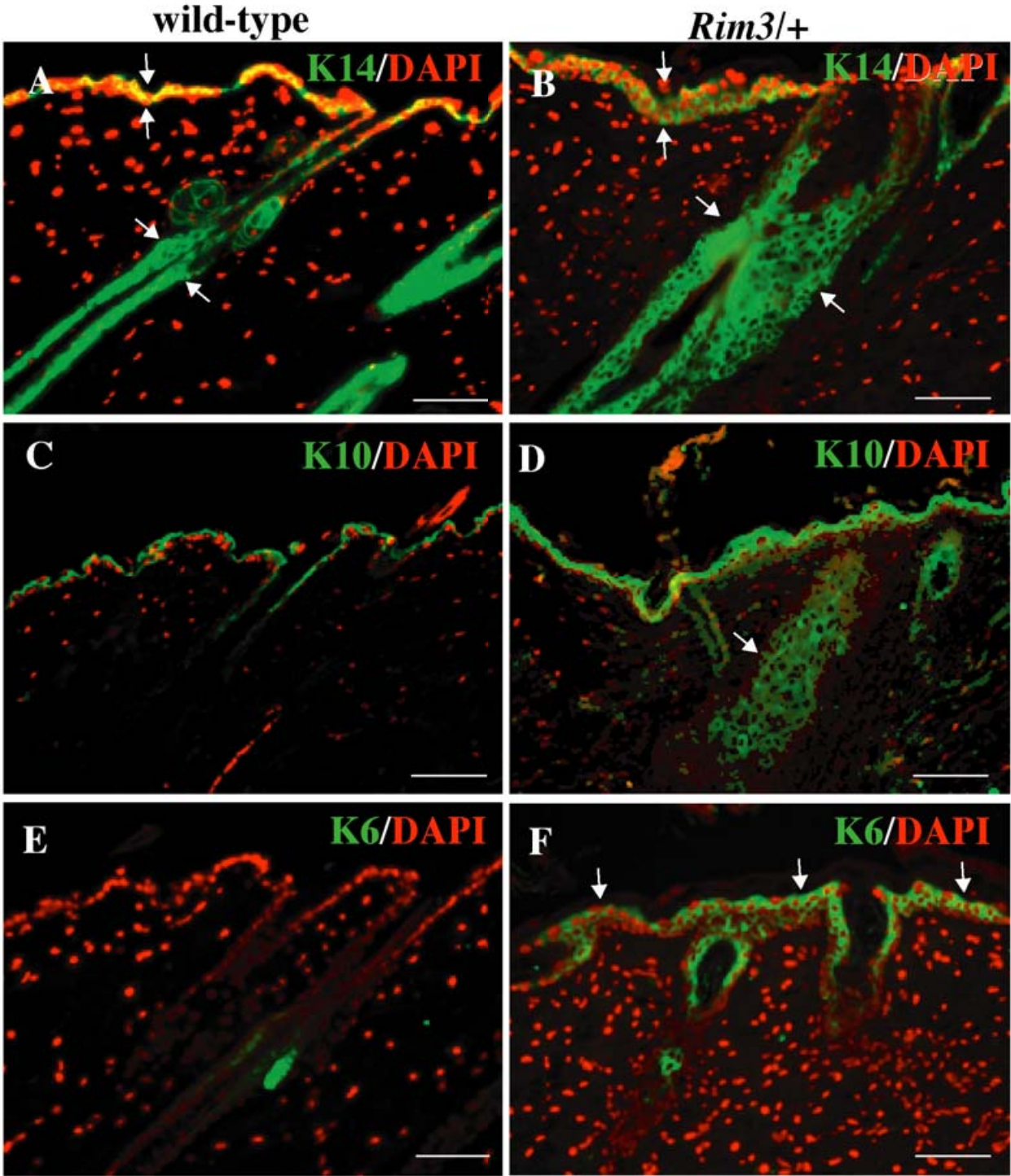


Figure 7. Proliferation of the epidermal cells in *Rim3*^{+/+} mouse. To analyze of proliferation of epidermal cells, incorporation of BrdU in basal layer and hair follicles was assayed with anti-BrdU antibody. In 3 months-old *Rim3*^{+/+} mouse, an increased number of BrdU-positive cells were observed in the upper hair follicles and the interfollicular epidermis (arrows in B), as compared with that of the wild-type mouse (arrows in A). Scale bar is 50 μ m.

Figure 7

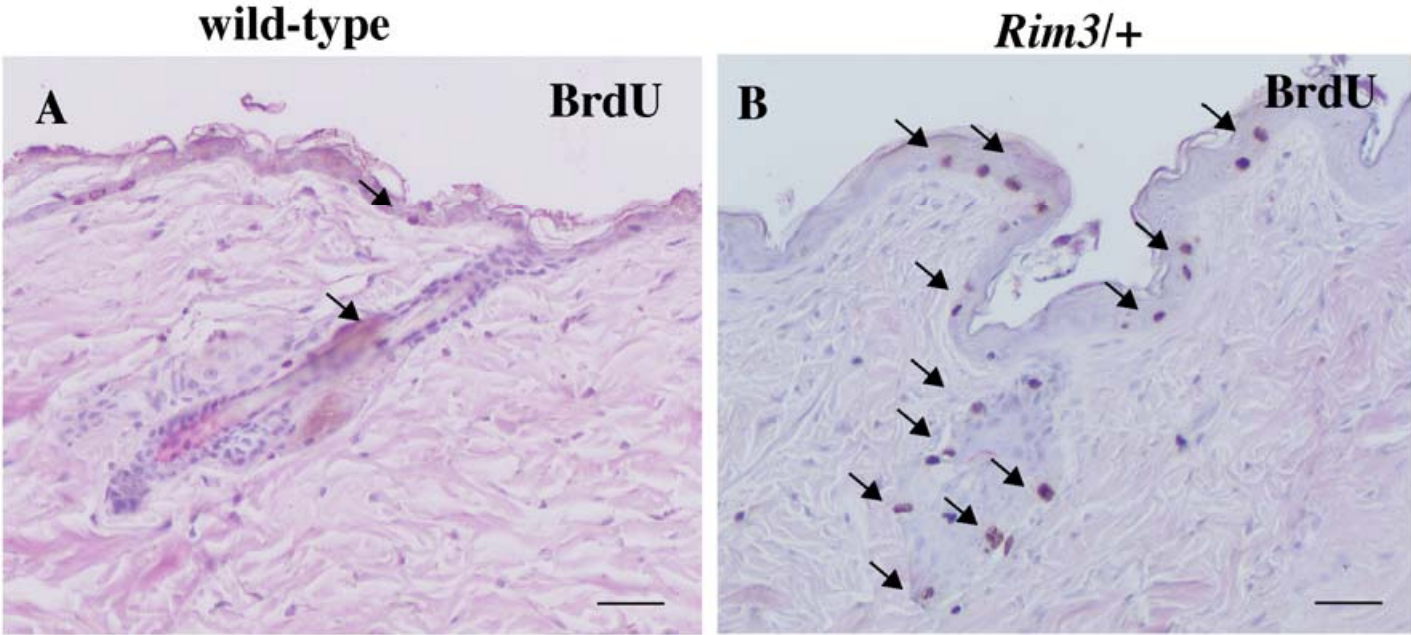


Figure 8. Detection of sebocytes in sebaceous glands by Oil Red O staining. Cryosections of dorsal skins of the wild-type (A) and *Rim3*^{+/+} mice (B) at 3 months of age were stained with Oil Red O and Hematoxylin. Sebaceous glands reside in the upper portion of bulge in the wild-type mouse (arrows in A). No sebocyte was observed in *Rim3*^{+/+} mouse (B). Scale bar is 50 μ m.

Figure 8

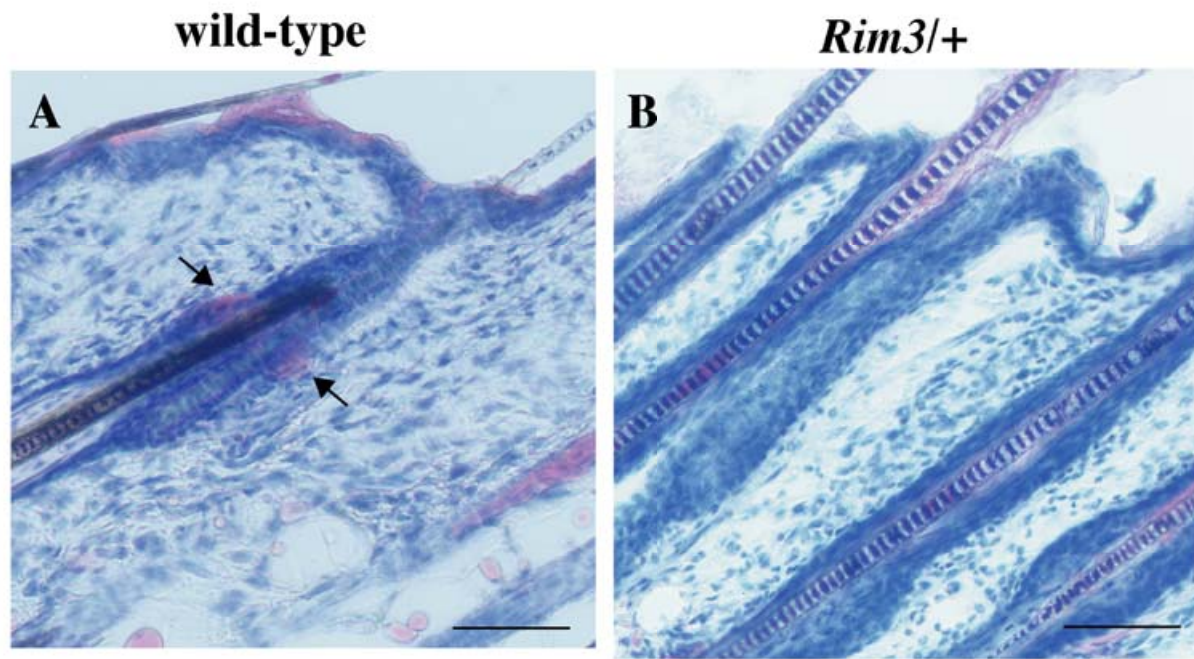


Figure 9. Localization of GsdmA-1 and/or GsdmA-3 proteins revealed by Immunohistochemical analysis. Sagittal paraffin sections of dorsal skin of the wild-type (A and C) and *Rim3*^{+/+} mice (B and D) at 9 days after birth were stained with anti-GsdmA antibody. This antibody recognizes both GsdmA-1 and GsdmA-3 protein. The green signal depicts the staining of the antibody, and the red DAPI DNA staining (A-D). High magnification of A and B were shown in C and D, respectively. The results of analysis using confocal microscopy were shown in E, F and G. The broken line indicates basal lamina in Figure C and D. Scale bar is 50 μ m.

Figure 9

wild-type

Rim3/+

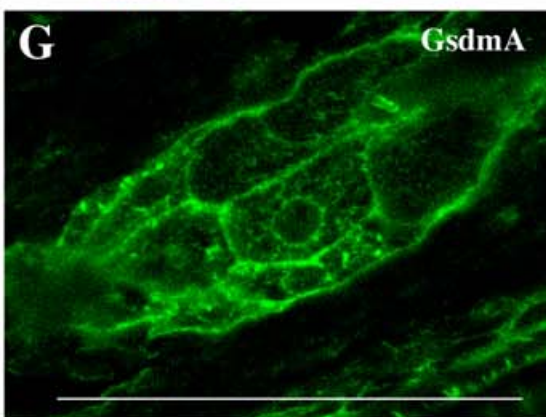
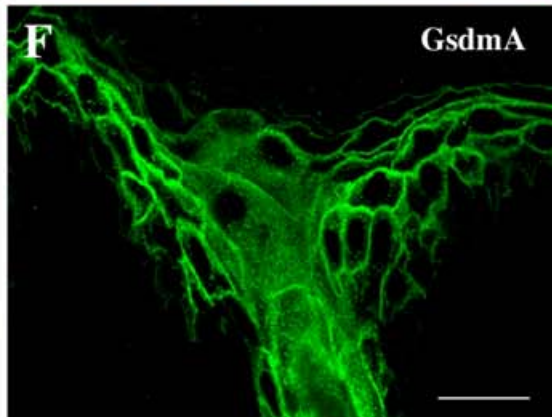
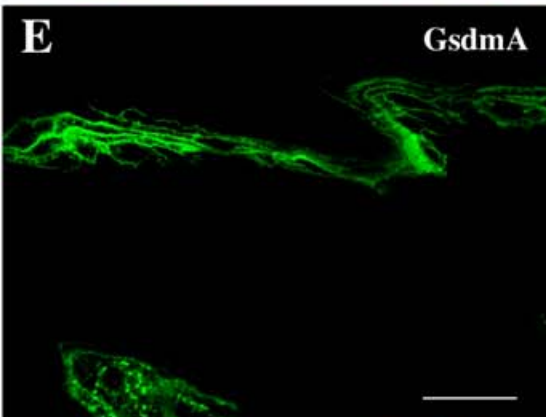
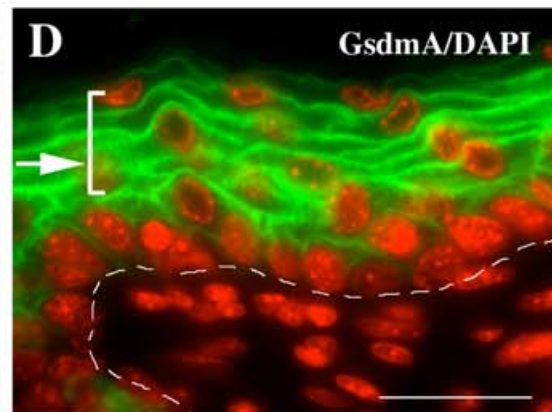
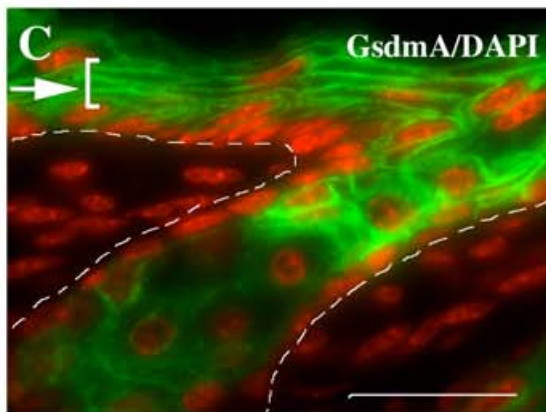
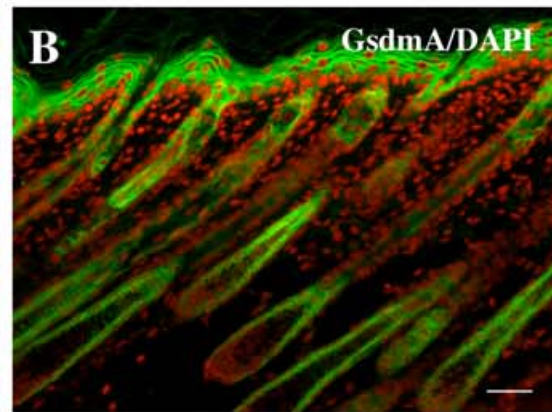
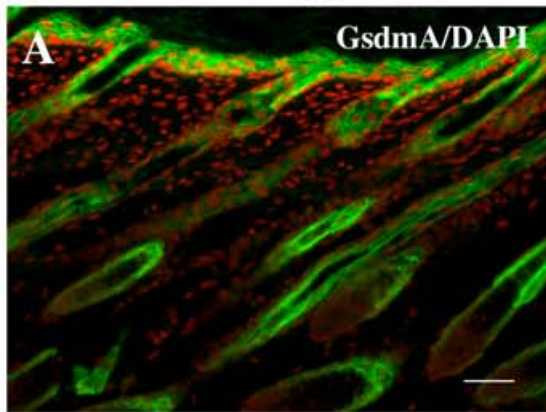


Figure 10. Localization of the GsdmA-1 and /or GsdmA-3 proteins and proliferating cells. The signals of GsdmA-1 and/or GsdmA-3 proteins (green) were not overlapped with the signals of BrdU (magenta) in the epidermis of the wild-type (A) and *Rim3/+* (B). Scale bar is 50 μm .

Figure 10

wild-type

Rim3/+

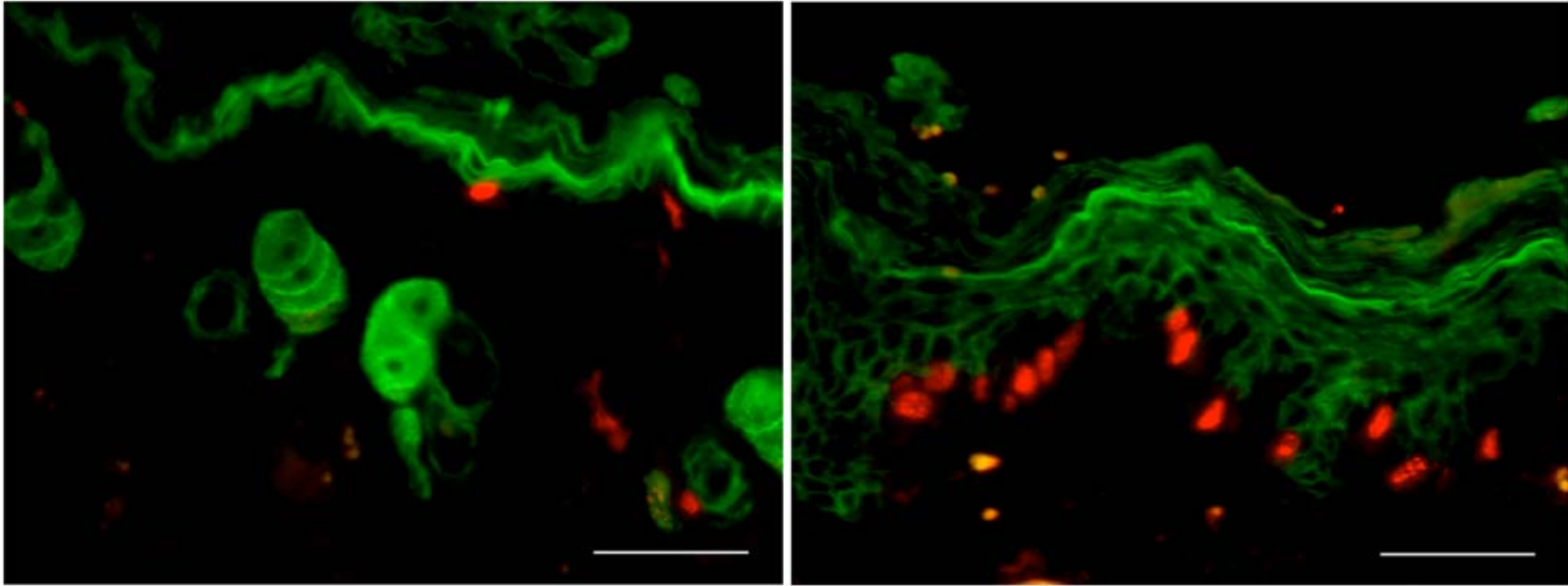


Figure 11. Fine analysis of location of the GsdmA proteins by immunoelectron microscopy. Immunoelectron microscopic horizontal images of hair follicle (A, B and C) and vertical images of sebaceous gland (D and E) are shown. B, C and E are higher magnifications of the insets in A and D, respectively. The plasma membrane of Henle's (He) layer in the inner root sheath (IRS) is labeled with gold particles (arrows in B). Particles are observed in vesicles (arrowheads in B) and organelles in the Huxley's (Hu) layer (arrows in C). In sebocytes, particles were specifically detected in unknown high-density granules (arrow in D, E). ORS, outer root sheath; IRS, inner root sheath; He, Henle's layer; Hu, Huxley's layer; HS, hair shaft; Th, trichohyalin granule; Nu, nuclear; SC, sebocyte.

Figure 11

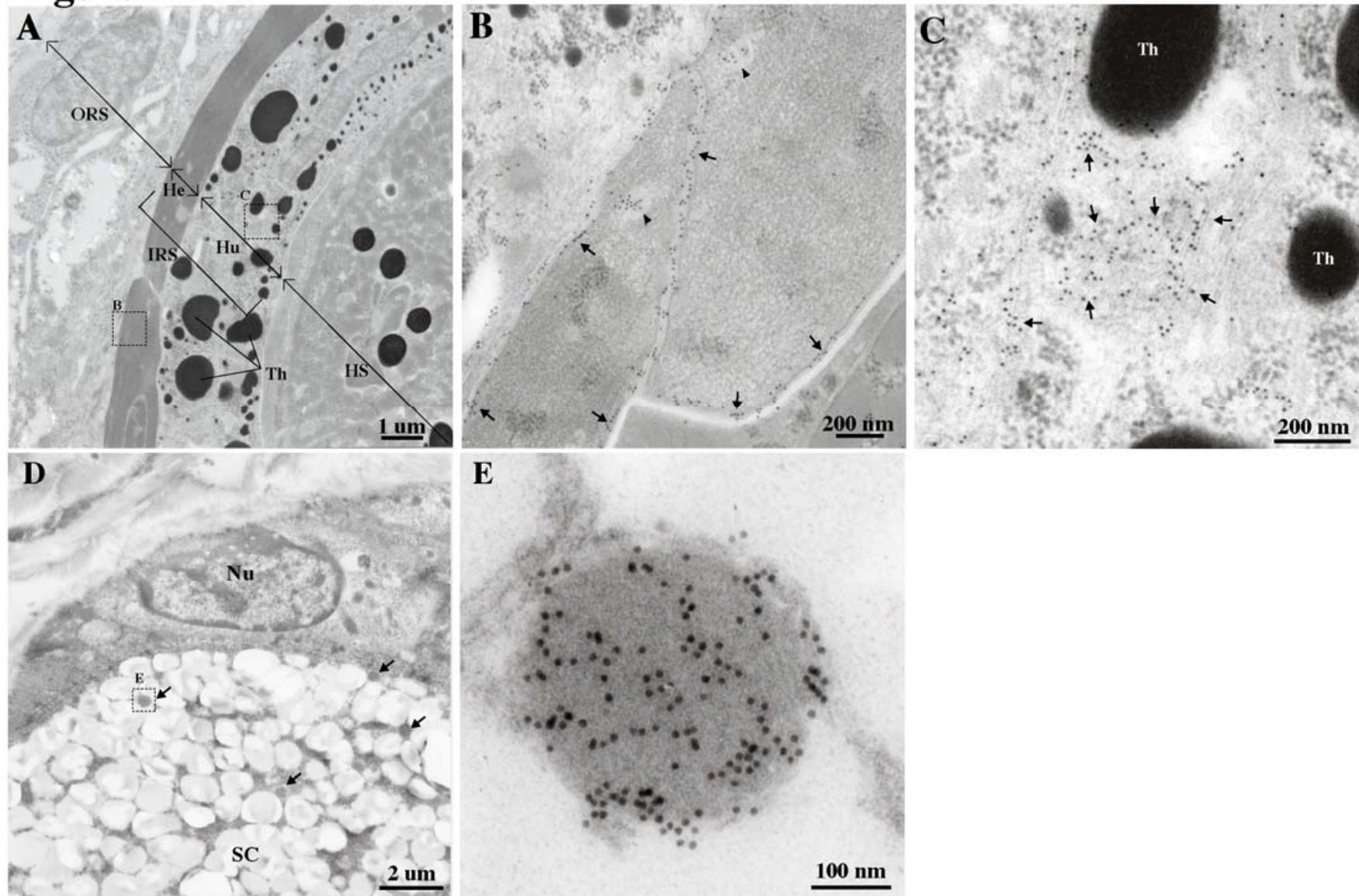
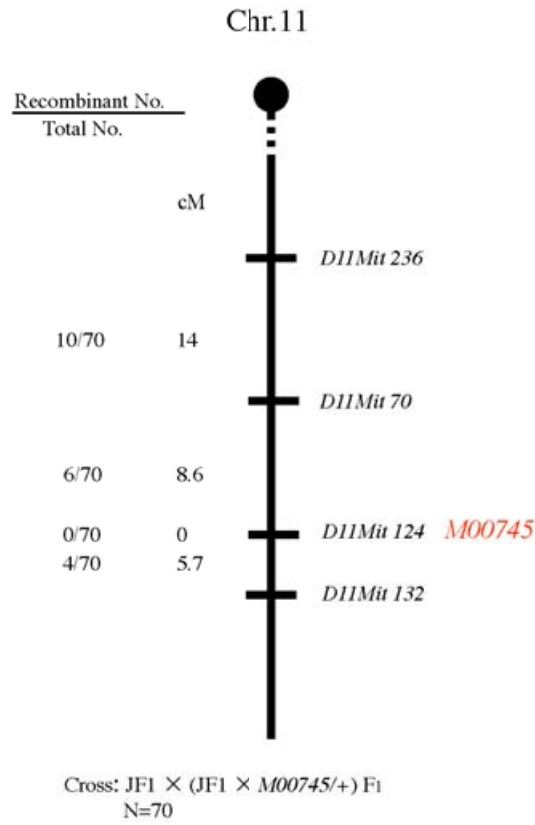


Figure 12. Gene mapping of *M00745* and identification of mutation in *GsdmA-3*. (A) Genetic map of *M00745*. Microsatellite markers used in the linkage analysis are shown at the right side of the map. *M00745* was mapped to the region linked to *D11Mit124* and the *GsdmA* cluster in chromosome 11. (B) Sequence analysis of *GsdmA-3* in *M00745* mutant mice. *M00745* has a single base substitution, T1408A, which caused nonsense mutation, 442Tyrosine to Stop codon.

Figure 12

(A)



(B)

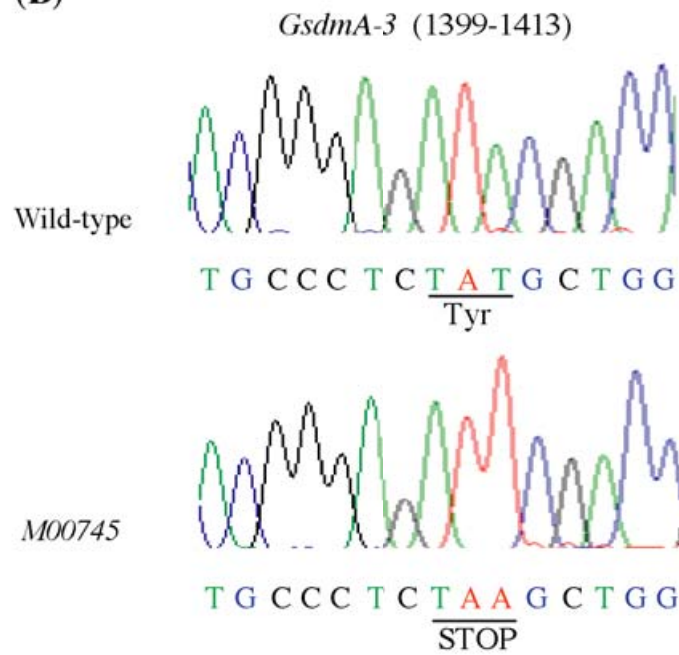


Figure 13. Histological analysis of the epidermis of *M00745/+* and *Rim3/+* mice. Sagittal sections of dorsal skin of 1 month (A and B) and 10 months (C and D) old *M00745/+* and *Rim3/+* mice were stained with Hematoxylin and Eosin. Although degenerated hair follicles, atrophy of sebaceous glands, and hyperproliferation of epidermis and hair follicles were commonly observed in the both mutant mice, the epidermis of the *M00745/+* mice was thicker than that of *Rim3/+* through the all ages. Scale bar is 50 μm .

Figure 13

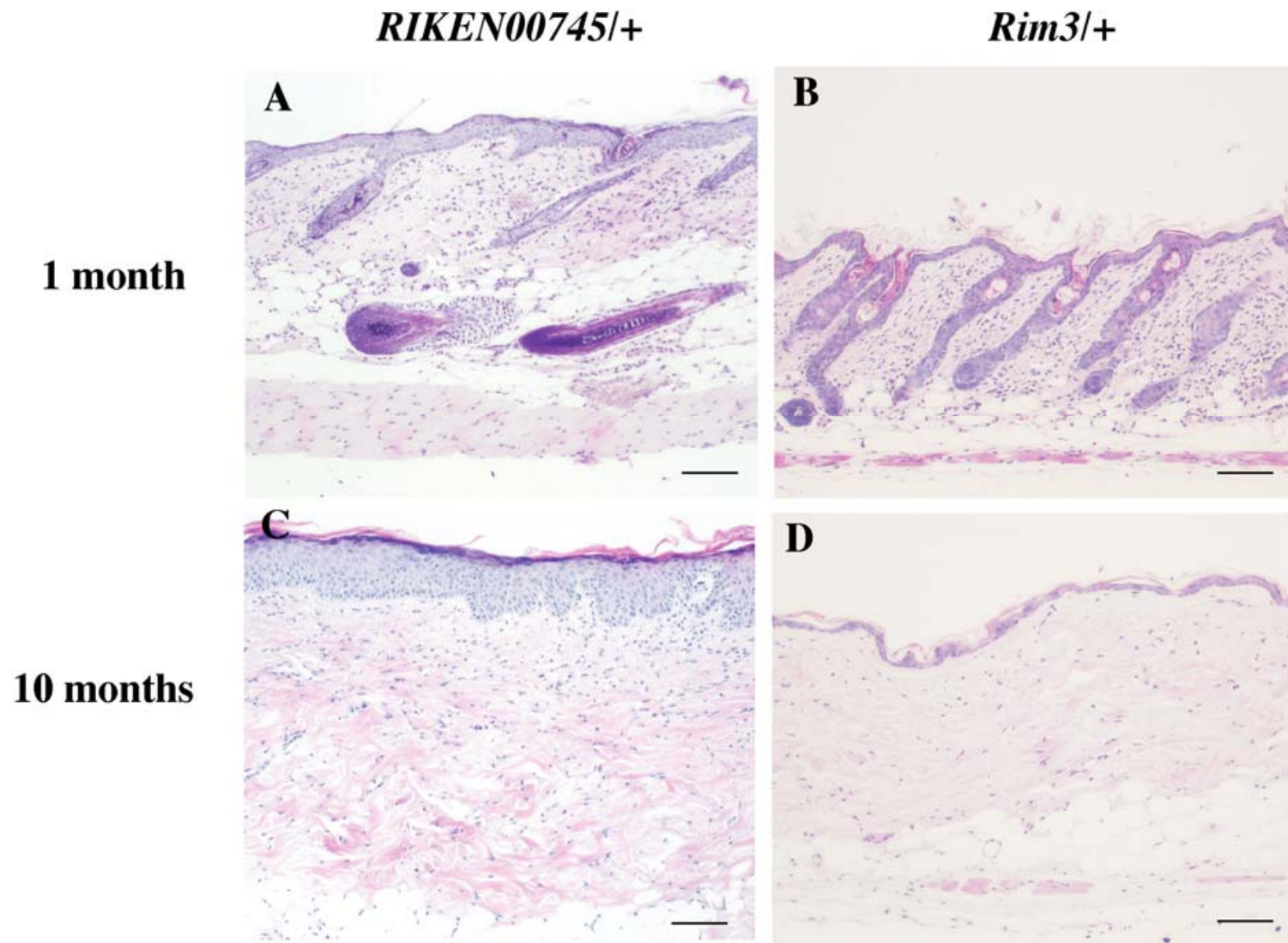


Figure 14. Late-onset corneal opacity in *Rim3*^{+/+} mouse. Typical gloss phenotype of the cornea of 1 month (A and B), 3 months (C and D) and 10 months (E, F and G) old wild-type (A, C and E), *Rim3*^{+/+} (B, D and F) and *M00745*^{+/+} (G) mice. At 3 months of age, the cornea of *Rim3*^{+/+} mouse showed mild opacity (D). At 10 months of age, the phenotype became much severe. The corneal epithelium exhibited hyperkeratization (F). *M00745*^{+/+} mice showed no corneal opacity even at 10 month of age (G).

Figure 14

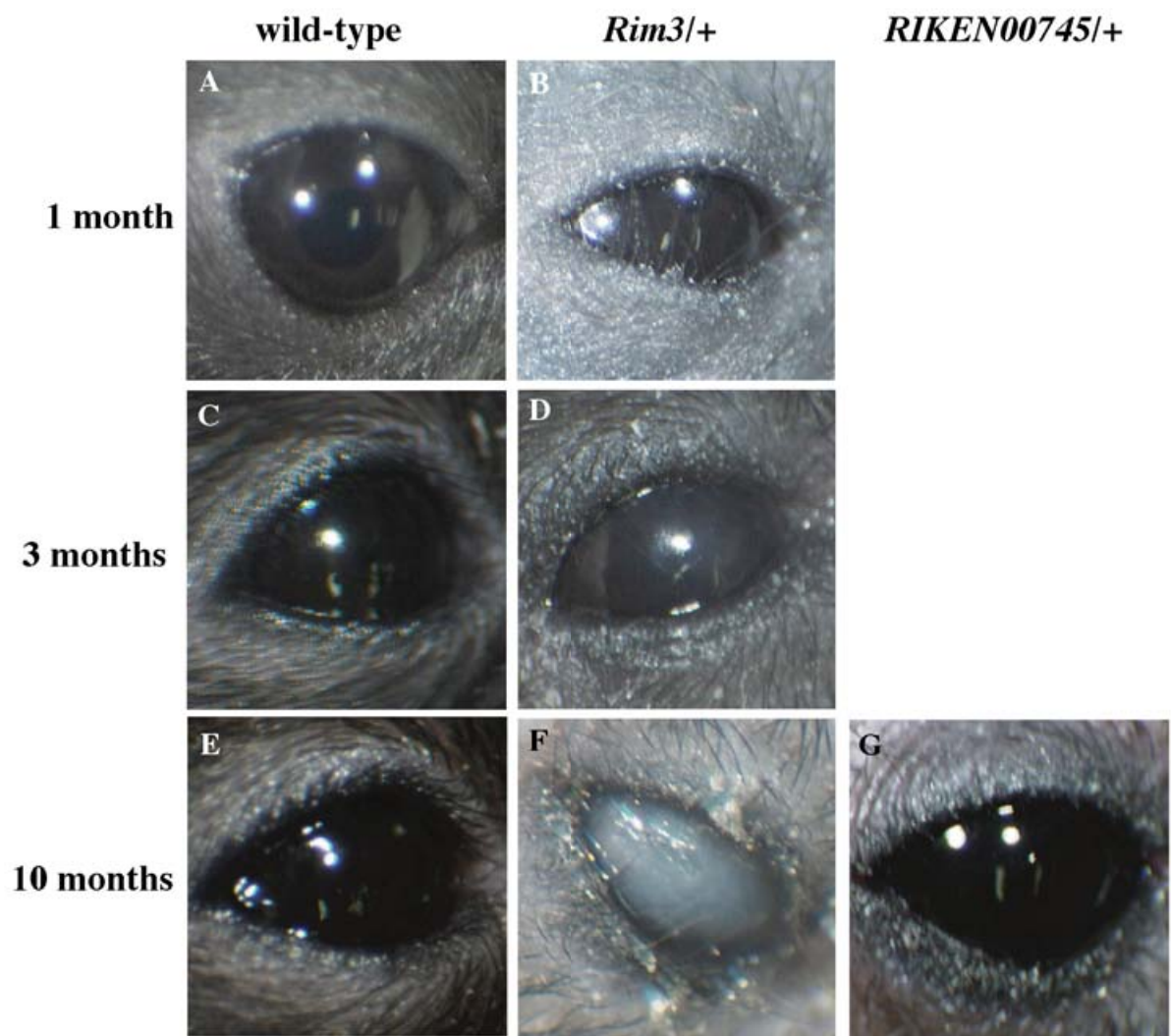


Figure 15. Histological analysis of meibomian glands in *Rim3/+* and *M00745/+* mice. Sagittal sections of upper eyelids of 1 month (A and B), 3 months (C and D) and 10 months (E, F, G and H) old wild-type and *Rim3/+* and *M00745/+* mice were stained with Hematoxylin and Eosin. In the wild-type mouse (A, C and E), meibomian glands have lobular cells (black arrows) containing meibum and are separated from hair follicles. In the *Rim3/+* mouse, the ductal epithelium of meibomian glands show hyperplasia (asterisks in B, D and F). There are few lobular cells at 3 months of age and no lobular cells except for cysts are observed at 10 months of age (white arrows in D and F). At 10 months of age, *M00745/+* mouse have many lobular cells as the wild-type mouse (black arrows in G and H), but the morphology of meibomian glands is abnormal and cysts are observed (white arrows in G). Ectopic hair-like structure is observed in highly magnified image of the meibomian glands of 10 months-old *M00745/+* mouse (white arrowheads in H). dc, duct; hf, hair follicle. Scale bar is 100 μ m.

Figure 15

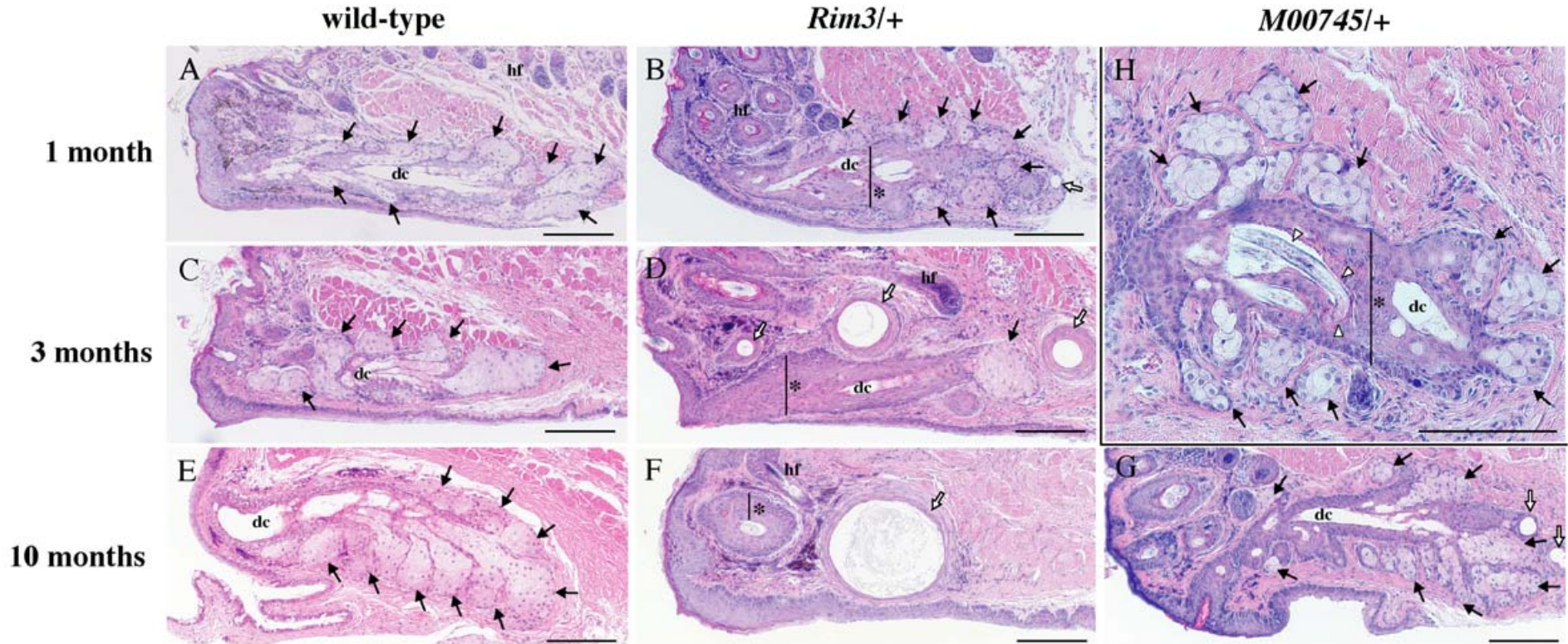
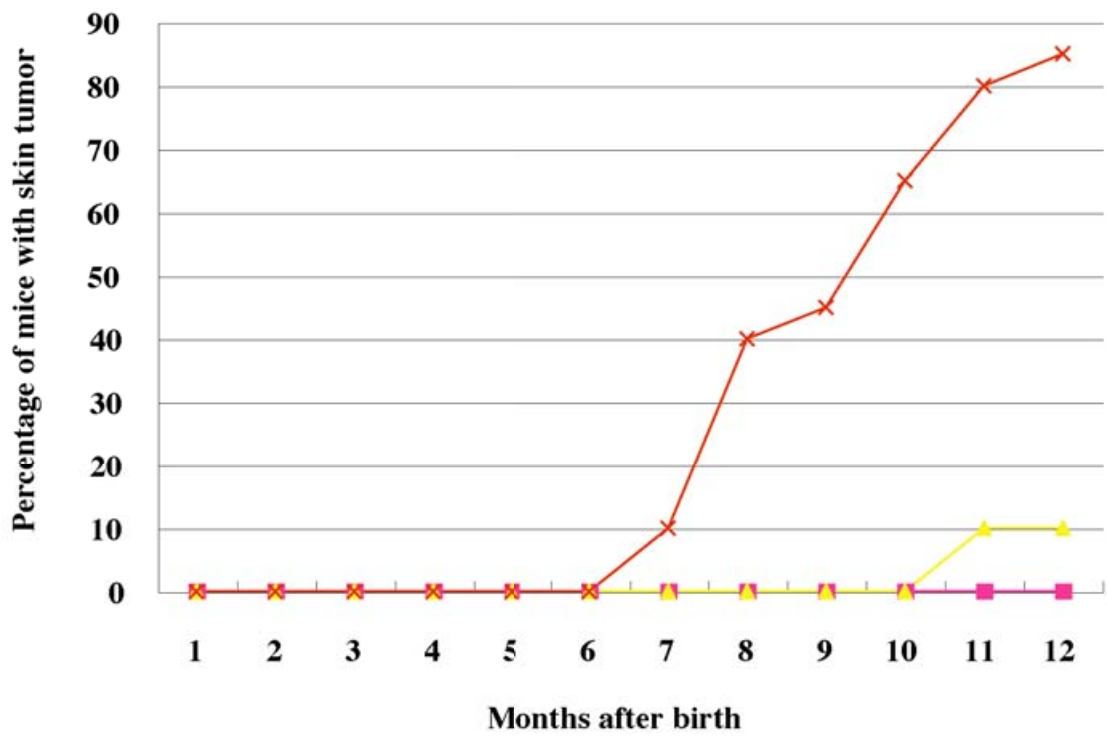


Figure 16. Cumulative incidence of skin tumors in mice heterozygous both for the *Rim3* and *Trp53* KO (*p53*) alleles. Percentage of mice that developed skin tumors were monitored from 1 month of age to 12 months of age. Blue line, wild-type mice (*GsdmA-3*^{+/+}; *Trp53*^{+/+}); pink line, *Trp53* heterozygous mice (*GsdmA-3*^{+/+}; *Trp53*^{+/-}); yellow line, *Rim3*^{+/+} mice (*GsdmA-3*^{Rim3}^{+/+}; *Trp53*^{+/+}); red line, double heterozygous (*GsdmA-3*^{Rim3}^{+/+}; *Trp53*^{+/-}) mice. Numbers in the parentheses were mice used in the test.

Figure 16



(n=21) —◆— *GsdmA-3^{+/+}; Trp53^{+/+}*

(n=20) —■— *GsdmA-3^{+/+}; Trp53^{-/+}*

(n=19) —▲— *GsdmA-3^{Rim3}/+; Trp53^{+/+}*

(n=21) —×— *GsdmA-3^{Rim3}/+; Trp53^{-/+}*

Figure 17. Macroscopic and histological analysis of skin tumors developed in the double heterozygous (*GsdmA-3^{Rim3}/+*; *Trp53^{+/-}*) mice. The macroscopic views (A-E) and the histology of skin tumors (F-J) are shown. The section of the SCC (D) is shown in F. Highly magnified images of the insets in F are shown in G-I. Epidermal layer (e, darker stain) is thickened and expanded with stratified squamous epithelium that is covered by massive amounts of dense layered keratin (k in F). The epidermis adjacent to SCC shows hyperplasia (G). The SCC exhibits dyskeratosis and proliferation of squamous cells with various size of nuclear (H) and formed many of horn pearls (arrow in I). Metastasis of SCC is observed in lymph node at the periphery of the SCC (J). In the lymph node, stratified epithelium (e) is embedded in lymphocytes (ly) and is well differentiated to keratin (k). White line in D indicates cut line of the section in F. In the section F, k, keratin; e, epidermis; ly, lymphocytes. Scale bar is 50 μm (G, H and I) and 100 μm (J).

Figure 17

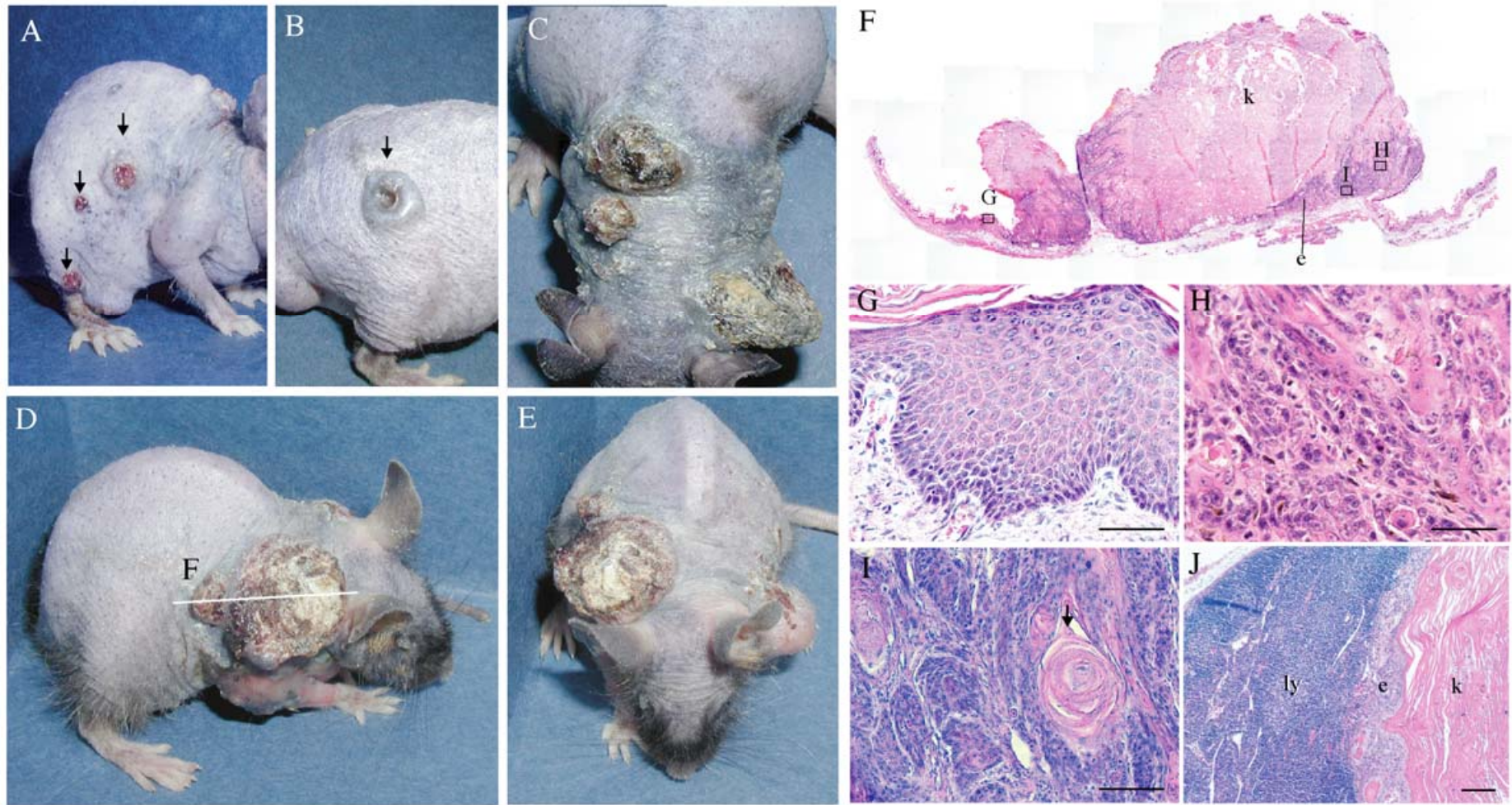


Figure 18. Localization of GsdmA-1/GSDMA and GsdmA-3 proteins in mouse and human normal tissues. The sections of wild-type mouse skin (A), normal human skin (B, C, D and E) were stained with Hematoxylin and Eosin (HE), and anti-GsdmA antibody. Arrowheads in B indicate melanocytes. e, epidermis; sb, sebocytes; hf, hair follicles; sg, sweat glands. Scale bar is 50 μ m.

Figure 18

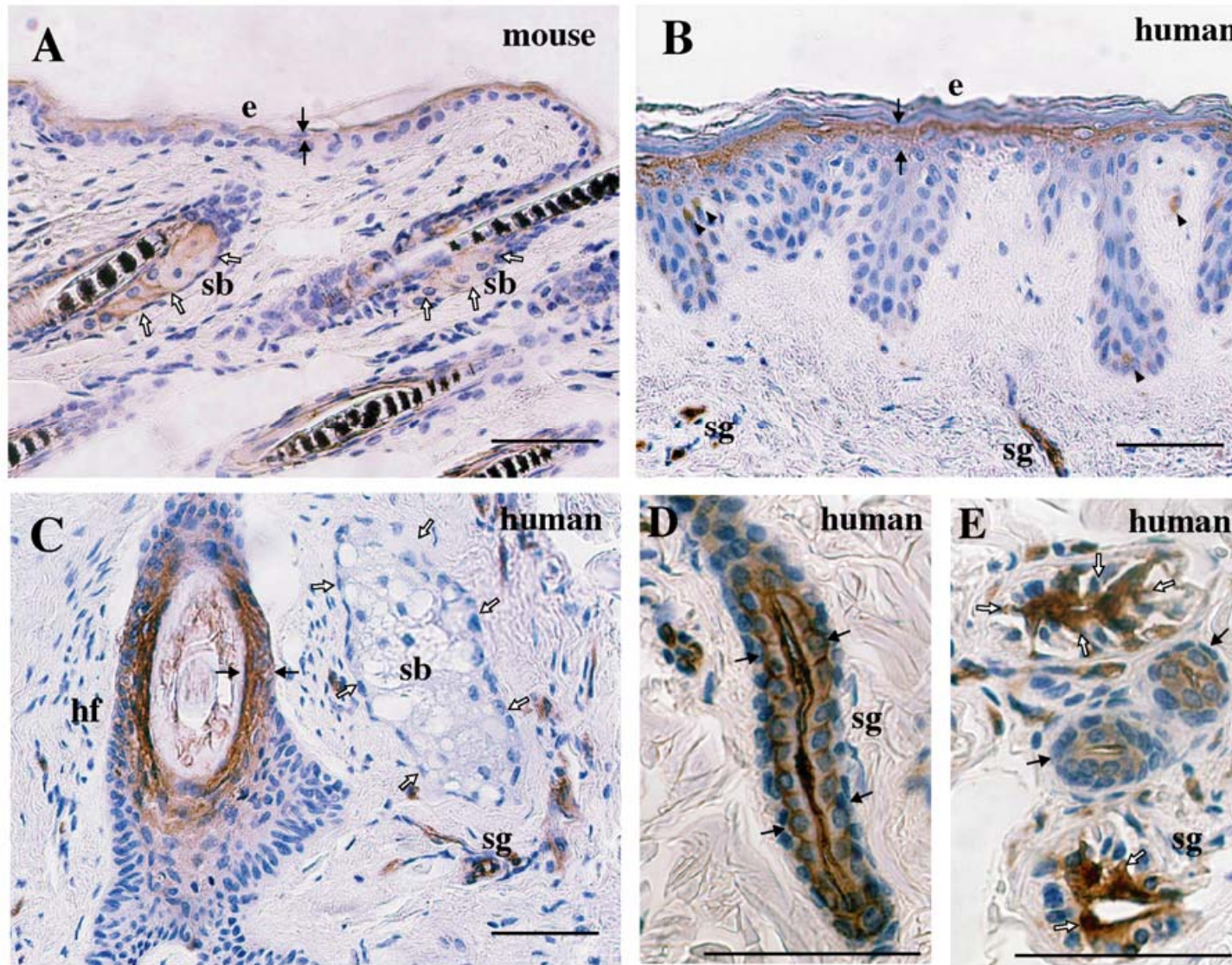


Figure 19. Localization of GsdmA-1/GSDMA and GsdmA-3 proteins in mouse and human skin tumors.

The sections of mouse SCC that developed in the double heterozygotes (A and B) and human SCC (C and D) were stained with Hematoxylin and Eosin (HE), and anti-GsdmA antibody. Scale bar is 50 μm .

Figure 19

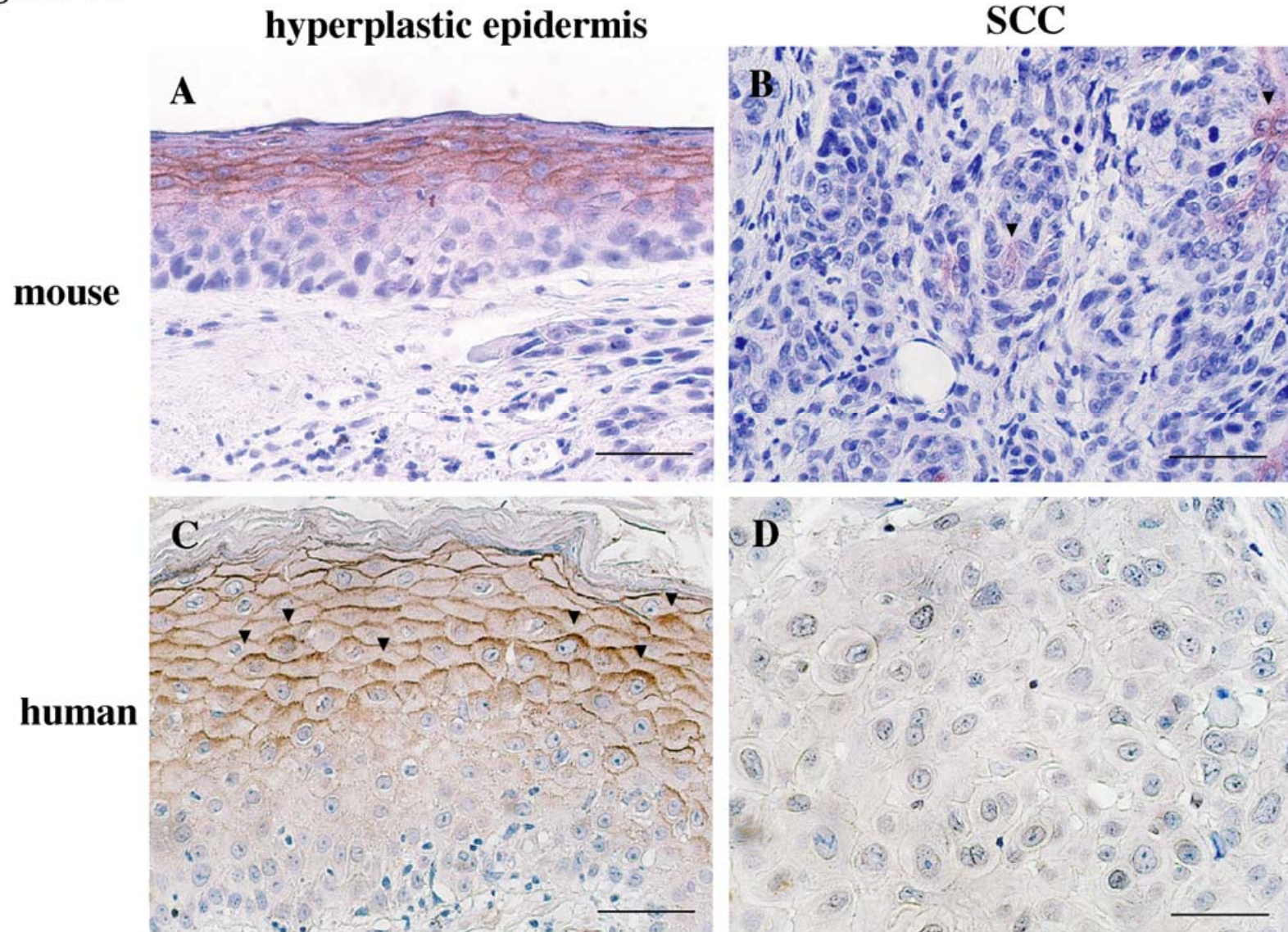


Figure 20. Localization pattern of GsdmA-1 and/or GsdmA-3 proteins in hyperplastic epidermis. Serial sections of hyperplastic epidermis in the double heterozygous mouse with SCC were stained with HE or the anti-GsdmA antibody. White arrowheads indicate basal cell layer. Bar with asterisk indicates differentiated cell layers. Black arrowheads indicate final differentiated cell layers. The broken line indicates basal lamina. Scale bar is 50 μm .

Figure 20

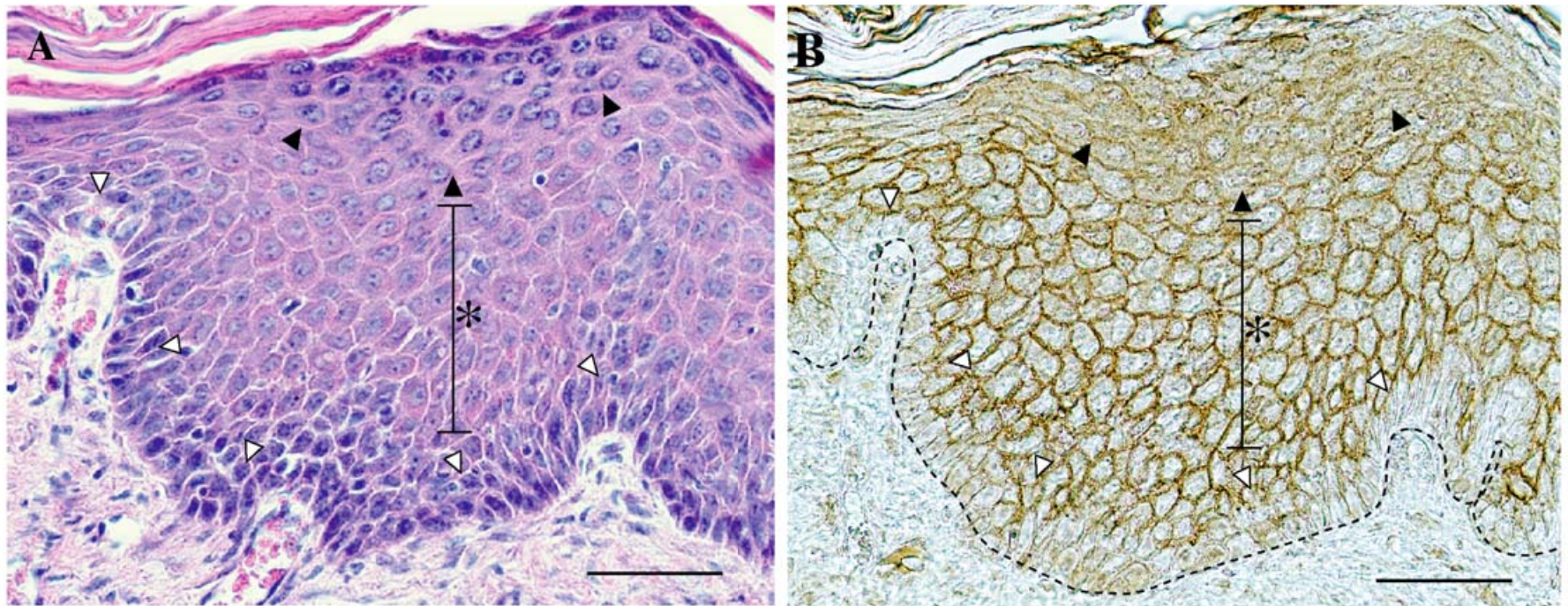
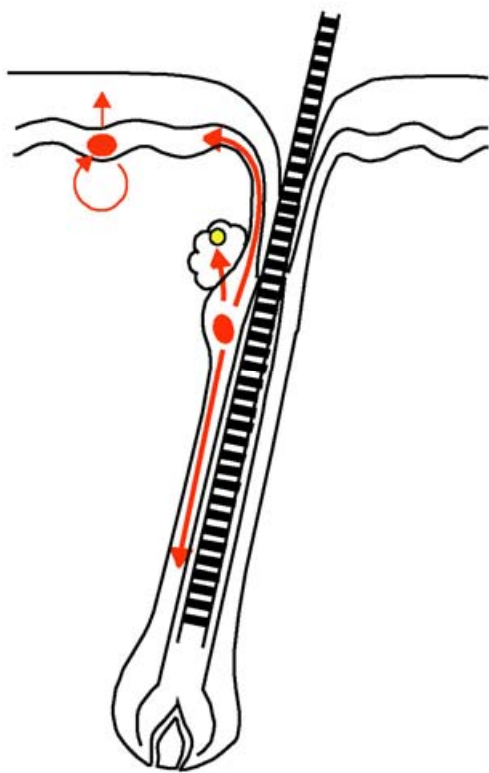
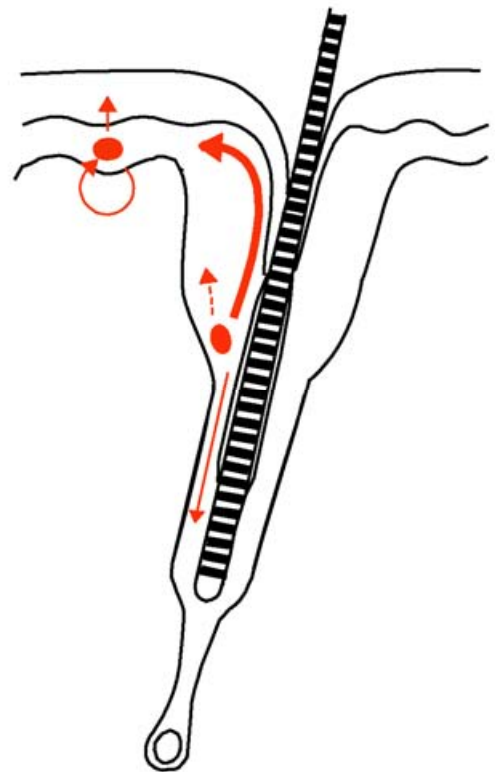


Figure 21. Summary of the phenotype of the *Rim3* mutant. In wild-type epidermis, bulge stem cells upwardly migrate to interfollicular epidermis and downwardly migrate to lower follicular epidermis. In *Rim3*^{+/+} epidermis, the bulge stem cells predominantly migrate to the interfollicular epidermis, resulting in abnormal differentiation and proliferation of the upper follicular epidermis.

Figure 21



wild-type



Rim3/+

Figure 22. Feedback model of proliferation-suppression of stem cells by differentiated supra basal epidermis. In wild-type mice, differentiated epidermal cells in the supra basal layer negatively regulate the proliferation of the stem cells in the basal layer. In *Rim3*^{+/+} mice, abnormal differentiated cells lose the suppressive activity, resulting in hyperproliferation of stem cells.

Figure 22

